Biological, Medical Devices and Systems

A Portable Bioimpedance Spectroscopy Measurement System for Congestive Heart Failure Management

M. Delano, C. G. Sodini
Sponsorship: Medical Electronic Device Realization Center, Analog Devices

An estimated five million people are currently diagnosed with congestive heart failure (CHF) in the United States, with over 400,000 new diagnoses annually. Almost one in two patients will be readmitted to the hospital within four to six months of discharge. Readmissions can occur when the patient becomes fluid-overloaded due to poor medication and/or diet compliance, among other reasons. Up to 50% of these early re-admissions may be prevented if symptoms are recognized early enough and medication and diet compliance improve.

CHF is frequently associated with significant fluid retention in the lungs and legs. Bioimpedance techniques can be used to estimate the fluid levels in a patient non-invasively. These measurements have been shown to be predictive of heart failure decompensation up to 14 days before an event occurs We have developed a portable bioimpedance system that can measure body impedance from 1 kHz to 1 MHz. The system uses the magnitude-ratio and phase-difference detection (MRPDD) method to calculate the magnitude and phase of the measured impedance (see Figure 1). The system is enclosed in aluminum box (see Figure 2) and can be used with four co-axial cables. Each co-axial cable is actively driven by a screen driver circuit that reduces stray capacitance from the cables. Data from the device can be sent directly to a computer or transmitted over bluetooth (with lid off). The device has been characterized with RC networks and is being validated in healthy volunteers.

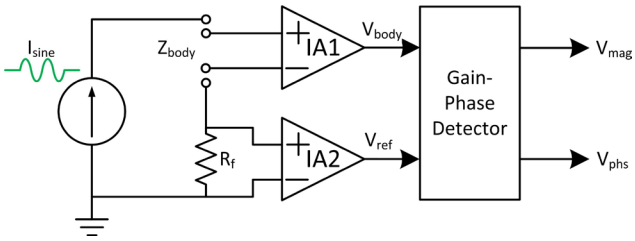

▲ Figure 1: A schematic overview of the MRPDD method. A fixed sinusoidal current is driven through the body and a sense resistor The voltage is amplified and measured by a Gain-Phase Detector chip (AD8302).

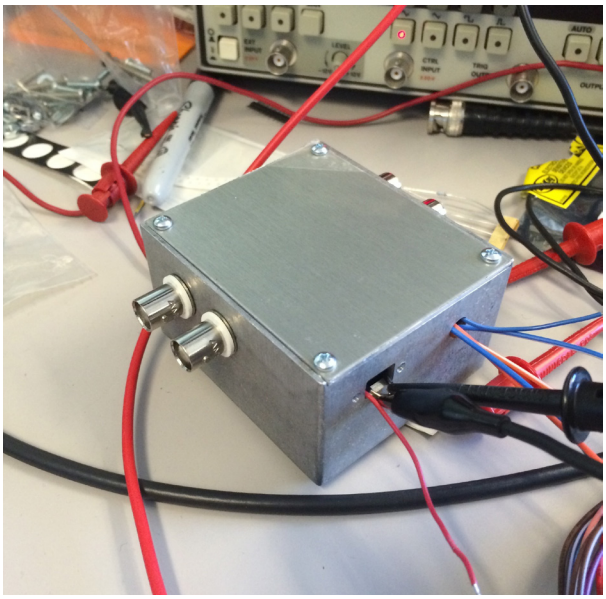

▲ Figure 2: The portable bioimpedance spectroscopy measurement system inside the enclosure.

FURTHER READING

- M. Delano and C. Sodini, "A Long Term Wearable Electrocardiogram Measurement System," in Body Sensor Networks Conference, 2013, pp. 1-6.
- E. Winokur, M. Delano, and C. Sodini, "A wearable cardiac monitor for long-term data acquisition and analysis," *IEEE Transactions on Biomedical Engineering*, vol. 60, pp. 189-92, January 2013.
- E. Winokur, D. He, and C. Sodini, "A wearable vital signs monitor at the ear for continuous heart rate and pulse transit time measurements," in *IEEE Engineering in Medicine and Biology Conference*, 2012, pp. 2724-2727.

Subdermal Implantable EEG Recorder and Seizure Detector

B. Do Valle, C. G. Sodini
Sponsorship: Center for Integrated Circuits and Systems

Epilepsy is a common chronic neurological disorder that affects about 1% of the world population. Although electroencephalogram (EEG) has been the chief modality in the diagnosis and treatment of epileptic disorders for more than half a century, long-term recordings (more than a few days) can be obtained only in hospital settings. Many patients, however, have intermittent seizures occurring far less frequently. Patients cannot come into the hospital for weeks in order for a seizure to be captured on EEG—a necessary prerequisite for making a definitive diagnosis, tailoring therapy, or even establishing the true rate of seizures.

This work aims to address this need by proposing a subdermal, implantable, eight-channel EEG recorder and seizure detector. The system will be implanted behind the patient's ear, as shown in Figure 1. It has two modes of operation: diagnosis and seizure counting. In the diagnosis mode, EEG is continuously recorded and transmitted to an external device. In the seizure-counting mode, the system uses a novel low-power algorithm to track the number of seizures a patient has over a given time period, providing doctors with a reliable count to help determine medication efficacy. This mode is especially important given the severity of antiepileptic drugs' side-effects.

An application-specific integrated circuit (ASIC) that implements the EEG recording and seizure detection algorithm was designed and fabricated in a 0.18 µm CMOS process. The ASIC, shown in Figure 2, includes eight EEG channels and was designed to minimize the system's power and size. The result is a power-efficient analog front end that requires 2.75 µW per channel in diagnosis mode and 0.84 µW per channel in seizure-counting mode. Both modes have an input referred noise of approximately 1.1 µVrms. The seizure detection algorithm has a sensitivity of 98.5%, a false alarm rate of 4.4 per hour, and a detection delay of 9.1 seconds. It consumes only 0.45 µW, which is over an order of magnitude less power than comparable algorithms.

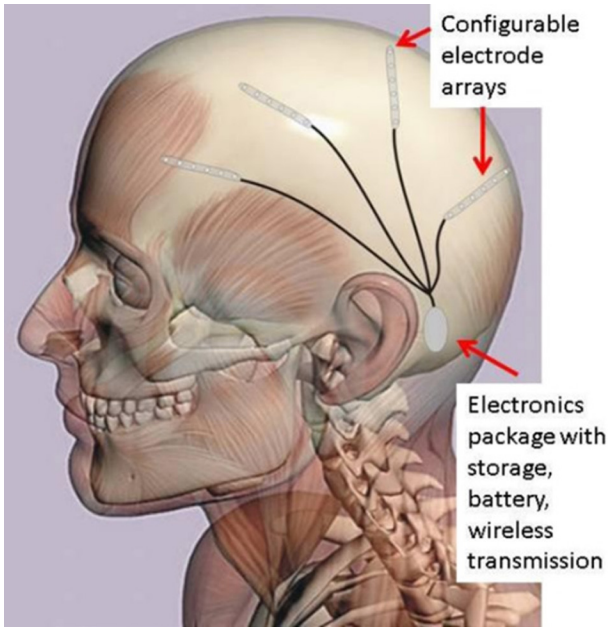

▲Figure 1: Implanted EEG system showing the location of the electronic package and electrodes.

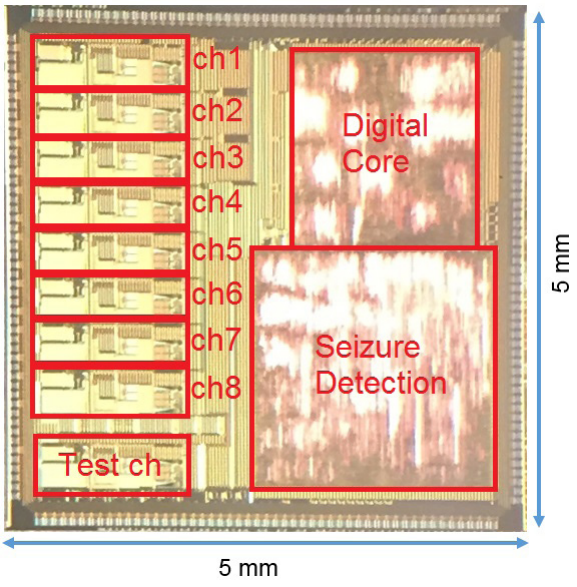

▲Figure 2: Die micrograph of the ASIC with circuit blocks labeled.

Continuous and Non-Invasive Blood Pressure Monitoring using Ultrasound

J. Seo, H.-S. Lee, C. G. Sodini
Sponsorship: Samsung Fellowship, Center for Integrated Circuits and Systems

An arterial blood pressure (ABP) waveform provides valuable information for treating cardiovascular diseases. The ABP waveform is usually obtained through a pressure transducer connected to an arterial catheter. Although this method is considered the gold standard, its disadvantage is invasive nature. The invasive nature not only increases various patients' risks but makes the usage of the ABP waveform for cardiovascular studies expensive. Therefore, reliable non-invasive ABP waveform estimation has been desired for a long time by medical communities. In that sense, medical ultrasound is an attractive imaging modality because it is inexpensive, free of radiation, cuff-less, and suitable for portable system implementation.

The proposed ultrasonic ABP monitoring is achieved by observing the pulsatile change of the cross-sectional area and identifying the elastic property of the arterial vessel, represented by the pulse wave velocity (PWV, the propagation speed of a pressure wave along an arterial tree) with a diastolic blood pressure measurement as a baseline. The PWV can be estimated by obtaining a flow-area plot and then measuring the slope of a linear part in the flow-area plot during a reflection-free period (e.g., the early systolic stage).

A prototype ultrasound device is designed to obtain both a blood flow waveform and a diameter waveform simultaneously to implement the proposed technique, shown in Figure 1. Clinical testing was conducted on nine healthy human subjects to demonstrate the feasibility of the proposed technique, which was previously tested in a phantom setup. Figure 2 presents a pressure waveform comparison between an ABP waveform obtained at a left middle finger and an estimated ABP waveform at the left common carotid artery from this method. The comparison shows good agreement although some degree of discrepancy is expected due to different measurement sites.

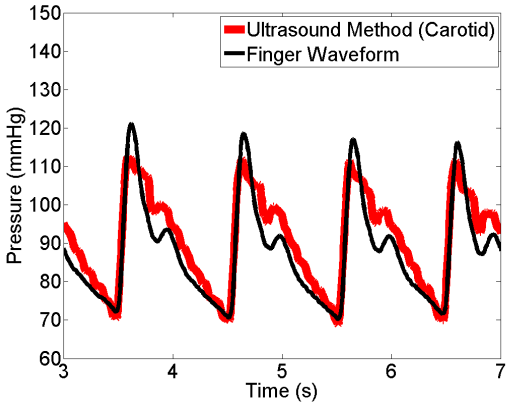

▲ Figure 1: A prototype PCB board design. The board drives ultrasound transducers, receives echoes, and process the voltage signal to implement the proposed method. The board is capable of streaming data to the PC over USB 2.0 interface with sufficient data rate for real-time data acquisition. The device has a portable form factor (14.7 cm×13.2 cm).

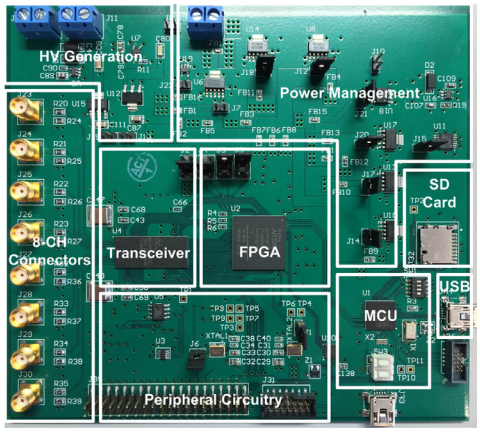

▲ Figure 2: Comparison of two blood pressure waveforms assuming diastolic blood pressures are constant over major arteries. An estimated carotid ABP waveform shows less augmented shape than the finger waveform as the finger waveform is more affected by pressure wave reflection from peripheries.

FURTHER READING

- J. Seo, S. J. Pietrangelo, H.-S. Lee, and C. G. Sodini, "Noninvasive arterial blood pressure waveform monitoring using two-element ultrasound system," *IEEE Transactions on Ultrasonics, Ferroelectrics, and Frequency Control*, vol. 62, no. 4, pp. 776-784, Apr. 2015.
- B. W. A. M. M. Beulen, N. Bijnens, G. G. Koutsouridis, P. J. Brands, M. C. M. Rutten, and F. N. Van De Vosse, "Toward noninvasive blood
- pressure assessment in arteries by using ultrasound," *Ultrasound in Medicine and Biology*, vol. 37, no. 5, pp. 788-797, May. 2011.

Body-Coupled Communication and Implants

G. S. Anderson, C. G. Sodini
Sponsorship: Google

Body-coupled communication (BCC) is achieved by creating a potential difference in one area of the body and sensing the resulting attenuated potential difference in another area of the body. To do this, the transmitter and receiver each have two electrodes that electrically connect to the body's conductive tissues beneath the epidermis. These connections can be formed either capacitively or galvanically. A capacitive link consists of the electrode forming one plate of a parallel plate capacitor while the conductive tissues form the other plate. A galvanic link is formed by directly putting the electrode or wire in the conductive tissue.

For an implant to communicate to a device outside the body using BCC, the channel utilizes both galvanic and capacitive links (capacitive for the device outside the body and galvanic for the implant). To test if this is possible a pork loin was used to simulate the conductive tissue of the body (see Figure 1). First, both the transmitter's and receiver's electrodes were connected to the pork loin using cardboard spacers between the pork loin and the electrodes, ensuring that both the transmitter and receiver would be capacitively coupled to the conductive tissue in the pork loin. Next the transmitter's output was connected to two alligator clips that were inserted into the pork-loin while the receiver was connected capacitively as before. This configuration simulates an implanted transmitter that is galvanically coupled to the conductive tissue, communicating with a receiver that is capacitively coupled. The results, shown in Figure 2, validate the predictions of the body model detailed in the further reading below.

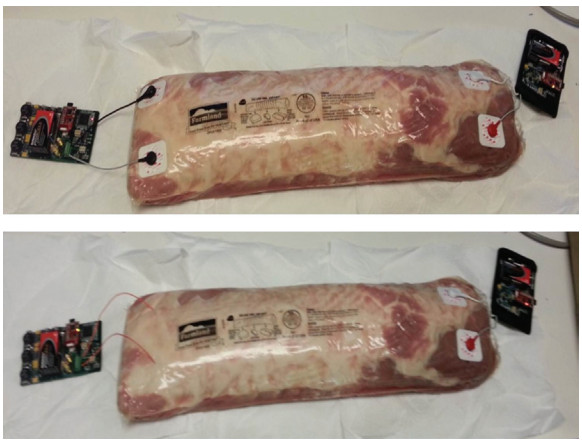

▲ Figure 1: A setup to test implants talking to devices outside the body using BCC.

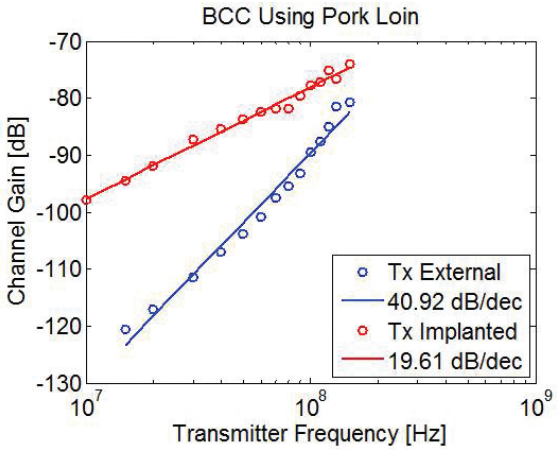

▲ Figure 2: BCC channel measurements.

FURTHER READING

- G. S.. Anderson and C. G. Sodini, "Body coupled communication: The channel and implantable sensors," *Body Sensor Networks (BSN), 2013 IEEE International Conference on* , vol., no., pp.1,5, 6-9 May 2013.
- T. G. Zimmerman, "Personal Area Networks (PAN): Near-field intrabody communication," Master's thesis, Massachusetts Institute of Technology, Cambridge, 1995.
- A. Fazzi et al., "A 2.75mW wideband correlation-based transceiver for body-coupled communication," *ISSCC Dig. Tech. Papers*, pp. 204-205, Feb. 2009.

Development of a Transcranial Doppler Ultrasound System

S. J. Pietrangelo, H.-S. Lee, C. G. Sodini
Sponsorship: MEDRC, Maxim Integrated

The central objective of critical care for patients affected by traumatic brain injury (TBI), cerebrovascular accident (i.e., stroke), and other neurovascular pathologies is to monitor patient state and provide suitable medical intervention to mitigate secondary injury and aid in recovery. Transcranial Doppler (TCD) sonography is a specialized Doppler ultrasound technique that allows characterization of blood flow from the basal intracerebral vessels. While several non-invasive cerebrovascular diagnostic modalities exist, including positron emission tomography (PET), computed tomography (CT), and magnetic resonance angiography (MRA), the use of TCD sonography is highly compelling for certain diagnostic needs due to its safety in prolonged studies, high temporal resolution, modest capital equipment costs, and relative portability.

Despite a growing list of potential diagnostic applications, several constraints – notably operator dependent measurement results, bulky instrumentation, and the need for manual vessel location – have generally confined the use of TCD ultrasound to highly-specific clinical environments (e.g., neurocritical care units and vascular laboratories). This project seeks to develop a low-power miniaturized TCD ultrasound system for measuring blood flow velocity at the middle cerebral artery (MCA) in support of continuous cerebrovascular monitoring.

The TCD ultrasound system shown in Figure 1 employs multi-channel transceiver electronics and a two-dimensional transducer array to enable steering of the ultrasound beam. Electronic beamformation allows for algorithmic vessel location and tracking, thereby obviating the need for manual transducer alignment and operator expertise. Figure 2 illustrates a conceptual TCD system for wearable, autonomous monitoring of cerebrovascular state.

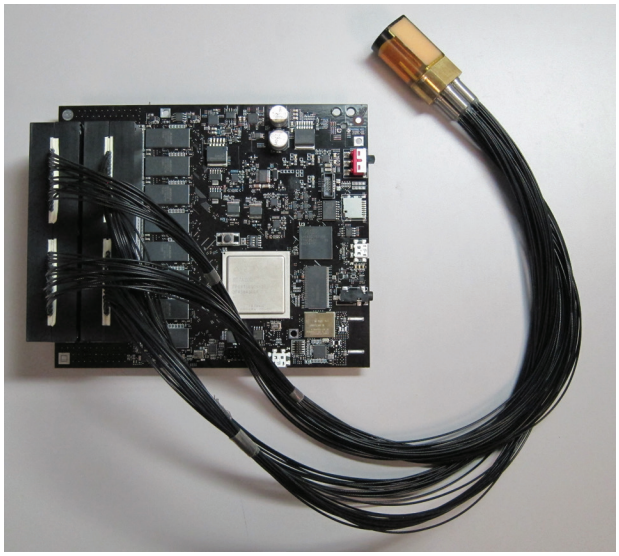

▲ Figure 1: TCD ultrasound electronics and transducer array.

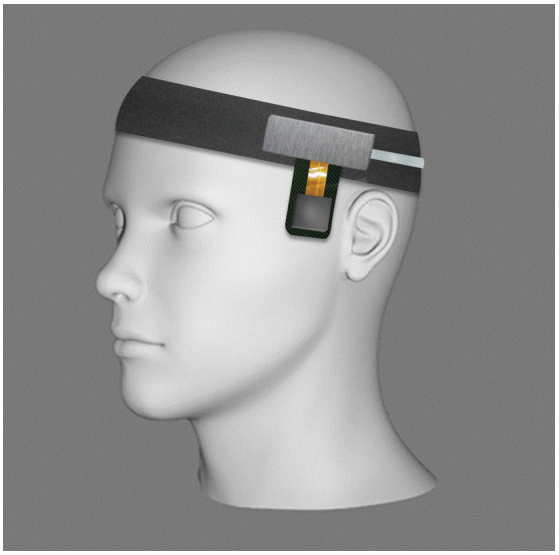

▲ Figure 2: Concept of a wearable TCD monitoring system with integrated ultrasound electronics.

FURTHER READING

- S. J. Pietrangelo, "An electronically steered, wearable transcranial Doppler ultrasound system," Master's thesis, Massachusetts Institute of Technology, Cambridge, 2013.

Stretchable Touch and Finger Position Sensors Molded into a Cloth Glove

M. D'Asaro, V. Bulović, J. H. Lang
Sponsorship: National Science Foundation Engineering Research Center for Sensorimotor Neural Engineering

The NSF Center for Sensorimotor Neural Engineering (CSNE) is working to reanimate a paralyzed human hand by recording and decoding motor intent from electrodes implanted in the brain and driving a spinal cord stimulator to induce the intended hand motion. To receive sensory feedback the user will wear a glove with integrated pressure and shear sensors, the data from which will be used to drive another set of implanted electrodes. This work aims to create a suitable sensing glove.

The glove will have pressure and shear sensors in the fingertips to restore the user's sense of touch plus finger position sensors to restore the user's intuition of finger position. For such a glove to be comfortable, the sensors and interconnects need to be small and compliant (flexible and stretchable). The sensors also need to be durable yet inexpensive to manufacture and replace when the glove wears out. To meet these requirements, sensors made from silicone rubber (PDMS) doped with carbon black (CB) are being explored. CB/PDMS is an inexpensive flexible and stretchable "smart material" that responds to mechanical deformation by increasing in resistance, thus forming a sensor. Fingertip pressure is sensed with a disk of CB/PDMS in the middle of the fingertip while finger curling is measured with a strip of CB/PDMS along the back of the finger, as in Figure 1. To electrically connect to the sensing CB/PDMS, a higher concentration CB/PDMS with added ~5 μm silver particles is used as a stretchable strain-insensitive conductor. Both materials can be molded directly into the nylon fabric of a commercial glove and adhere well.

Testing results from the pressure sensor are shown in Figure 2. Qualitative results from the finger curl sensor are encouraging. CB/PDMS shear sensors have been fabricated and tested but not yet integrated into a glove.

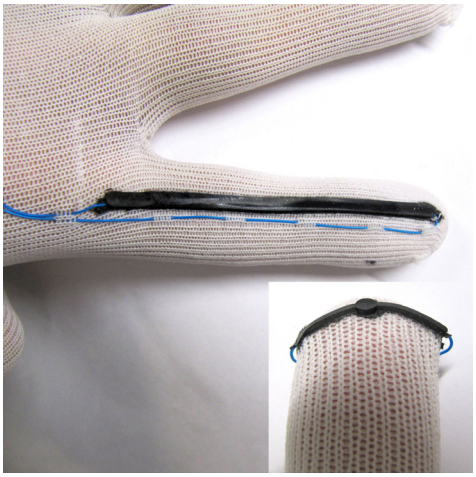

▲ Figure 1: Nylon glove with stretchable finger flex sensor molded into the back of the index finger. The inset shows a fingertip pressure sensor made with the same technology.

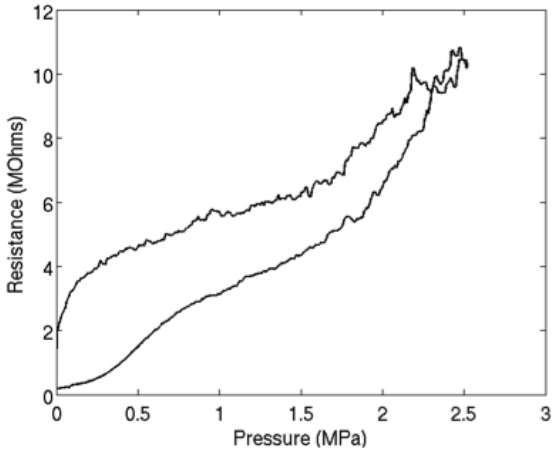

▲ Figure 2: Resistance of the fingertip pressure sensor versus applied pressure. The device is very sensitive, if hysteretic and nonlinear.

FURTHER READING

- R. Struempler and J. Glatz-Reichenbach, "Conducting polymer composites," *J. Electroceramics*, vol. 3 no. 4, pp. 329-346, Oct. 1999.
- M.-A. Lacasse, V. Duchaine, and C. Gosselin, "Characterization of the Electrical Resistance of Carbon-Black-Filled Silicone: Application to a Flexible and Stretchable Robot Skin," in Proc. 2010 *IEEE International Conference on Robotics and Automation (ICRA)*, pp. 4842-4848, 2010.
- F. M. Yaul and J. H. Lang, "A Flexible Underwater Pressure Sensor Array Using a Conductive Elastomer Strain Gauge," *Journal of Microelectromechanical Systems*, vol. 21, no. 4, Aug. 2012.

Piezoelectric Micro-machined Ultrasonic Transducer Array for Medical Imaging

K. M. Smyth, C. G. Sodini, S.-G. Kim
Sponsorship: Medical Electronic Device Realization Center, Analog Devices

Diagnostic medical ultrasound imaging is becoming increasingly widespread because it is relatively inexpensive, portable, compact, and non-invasive compared to other diagnostic scanning techniques. However, commercial realization of advanced imaging trends will require cost-effective, large-scale arrays of miniaturized elements, which are expensive to fabricate with the current bulk piezoelectric transducers. At high volume, micro-fabricated transducers based on micro-electromechanical (MEMS) technology are an array- compatible and low-cost option.

The piezoelectric micro-machined ultrasonic transducer (pMUT) is a promising alternative to previously proposed capacitive MUT devices since it does not suffer from electrostatic transduction limitations, including potentially unsafe high bias voltage, and nonlinearity. With more effective transformation via the piezoelectric effect, pMUTs have already demonstrated viability for deep penetration imaging via high acoustic pressure output. However, insufficient modeling has produced pMUT devices that often fall short of predictions, resulting in low electromechanical coupling and reduced bandwidth. With an improved modelling framework and optimization, pMUT based arrays have the potential for efficient low-power, high-pressure operation necessary for wearable applications.

Based on a high force output figure of merit, a 31-mode, lead zirconate titanate (PZT) -based pMUT plate cell design is selected. Our previous work developed and validated an analytical, electro-acoustic model of the single cell through experiment and finite element simulation. By leveraging and building on the validated single-cell model, we further optimized parallelized multi-cell elements to achieve high acoustic power and power efficiency. These elements are incorporated into 1D arrays (Figure 1) to demonstrate basic beamforming and image collection capabilities of a pMUT-based ultrasound system.

Current work focuses on fabrication of the pMUT arrays (Figure 2) using common micro-fabrication techniques including a PZT sol-gel deposition process. Work on model scaling to larger multi-cell systems and implementation of supporting electrical drive and receive circuits is also ongoing.

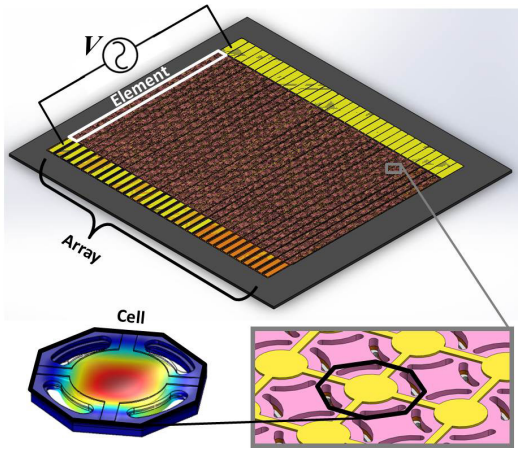

▲ Figure 1: Rendering of 1D pMUT array (top) where each element consists of many small pMUT cells (bottom right). Deflection of single cell based on piezo-acoustic finite element model simulated in COMSOL (bottom left).

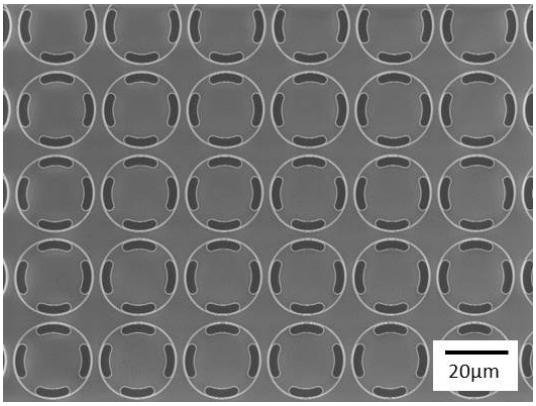

▲ Figure 2: Scanning electron microscope image of partially completed pMUT cells currently undergoing fabrication.

FURTHER READING

- K. Smyth, S. Bathurst, F. Sammoura, and S.-G. Kim, "Analytic Solution for N-electrode Actuated Piezoelectric Disk with Application to Piezoelectric Micromachined Ultrasonic Transducers," *IEEE Trans. Ultrason. Ferroelectr. Freq. Control*, vol. 60, no. 8, pp. 1756–1767, Aug. 2013.
- K. Smyth and S.-G. Kim, "Experiment and Simulation Validated Analytical Equivalent Circuit Model for Piezoelectric Micromachined Ultrasonic Transducers," *IEEE Trans. Ultrason. Ferroelectr. Freq. Control*, vol. 62, no. 4, pp. 744–765, April 2015.

Weighing Nanoparticles in Solution at the Attogram Scale

S. Olcum, N. Cermak, S. C. Wasserman, K. S. Christine, H. Atsumi, K. R. Payer, W. Shen, J. Lee, A. M. Belcher, S. N. Bhatia, S. R. Manalis
Sponsorship: ARO, CIMIT

Physical characterization of nanoparticles is required for a wide range of applications. Nanomechanical resonators can quantify the mass of individual particles with detection limits down to a single atom in vacuum. However, applications are limited because performance is severely degraded in solution. Suspended nanochannel resonators (SNRs) have opened up the possibility of achieving vacuum-level precision for samples in the aqueous environment, and a noise equivalent mass resolution of 27 attograms in 1-kHz bandwidth was previously achieved. We report on a series of advancements that have improved the resolution by more than 30-fold, to 0.85 attograms in the same bandwidth, approaching the thermomechanical noise limit and enabling precise quantification of particles down to 10 nm with a throughput of more than 18,000 particles per hour (Figure 1). We demonstrate the potential of this capability by comparing the mass distributions of exosomes produced by different cell types (Figure 2) and by characterizing the yield of self-assembled DNA nanoparticle structures.

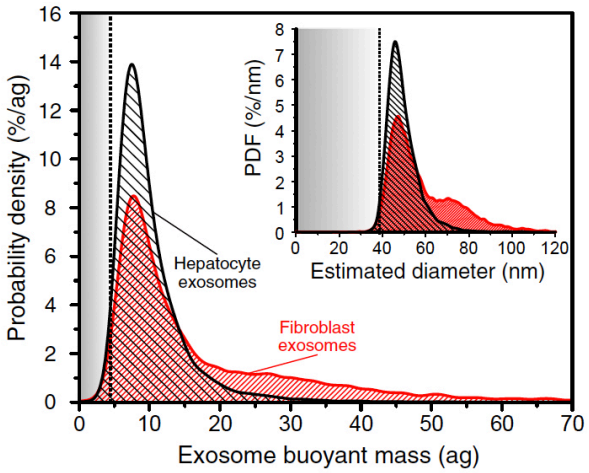

▲ Figure 1: Simplified schematic of SNR system; a positive-feedback loop keeps SNR in oscillation. An optical lever detects cantilever deflection, a photodetector circuit converts laser deflection to a voltage signal, a field programmable gate array (FPGA) delays the photodetector signal while also measuring oscillation frequency, and an amplifier drives the integrated piezoceramic actuator with the FPGA signal. Delay and oscillation amplitude are controlled by the FPGA to achieve minimum frequency noise. An oven-controlled crystal oscillator is used as clock source for the FPGA.

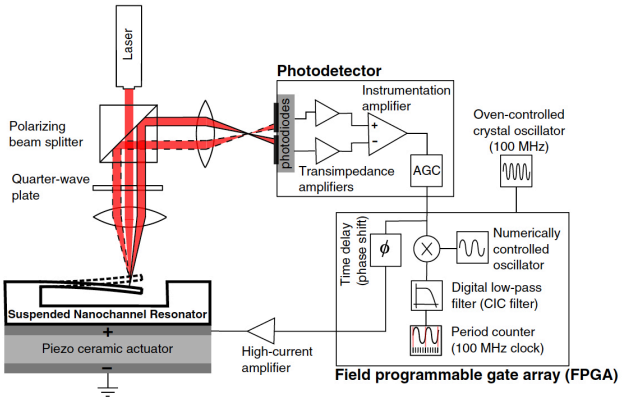

▲ Figure 2: Buoyant mass measurements of exosomes derived from different cell types. Buoyant mass distributions (kernel density estimates) of fibroblast-derived (red) and hepatocyte-derived (black) exosomal vesicles. Some 7,100 fibroblast exosomes and 9,600 hepatocyte exosomes are weighed using SNR in 65-min and 76-min experiments, respectively. Vertical dotted line depicts limit of detection as close to 5 ag. (Inset) Estimation of exosome diameter assumes spherical shape and constant exosome density of 1.16 g/mL throughout populations. Vertical dashed line indicates corresponding limit of mass detection as 39 nm.

FURTHER READING

- J. Lee, W. Shen, K. Payer, T. Burg, and S. R. Manalis, "Toward attogram mass measurements in solution with suspended nanochannel resonators," *Nano Letters*, vol. 10, no. 7, pp. 2537-2542, July 2010.
- S. Olcum, N. Cermak, S. C. Wasserman, K. S. Christine, H. Atsumi, K. R. Payer, W. Shen, J. Lee, A. M. Belcher, S. N. Bhatia, and S. R. Manalis, "Weighing Nanoparticles in Solution at the Attogram Scale," *Proc. National Academy of Sciences*, vol. 111, no. 4, pp. 1310–1315, Jan. 2014.

Microfluidic Blood Sorting for Improved Blood Quality over Prolonged Storage

C. Yu, S. Huang, H. W. Hou, J. Han
Sponsorship: Singapore-MIT Alliance for Research and Technology, DARPA Dialysis Like Therapeutics

Blood transfusion is one of the most common lifesaving medical therapies. According to the Food and Drug Administration regulation, refrigerated red blood cells (RBCs) can be stored up to 42 days. However, significant loss of RBC deformability typically occurs after 3 weeks of storage time due to ATP and 2,3-diphosphoglycerate (DPG) depletion. As a result, prolonged blood storage raises concerns of compromised blood quality and rapid RBC clearance post transfusion. However, studies suggest that not all stored RBCs are unfit for transfusion: only a subpopulation of transfused stored RBCs were rapidly cleared in mice, and the remaining transfused stored RBCs stayed in circulation in the same way as transfused fresh RBCs.

In our previous work, a novel microfluidic platform was employed to assess changes in human RBC deformability over prolonged storage periods. Banked RBCs were analyzed using a microfluidic deformability cytometer consisting of repeated bottleneck structures (Figure 1). Significant stiffening was observed between 21 and 28 days of storage (Figure 2a). For blood stored more than 4 weeks, a deformability-based microfluidic sorting device was applied to mechanically purify the old stored blood by enriching and separating the less deformable subpopulations. It was found that the side outlet was able to collect significantly stiffer and more fragile RBC subpopulations (Figure 2b).

To investigate whether there is a clinical benefit to transfusing the more deformable subpopulations of old stored blood, we aim to build a mouse model to assess the post-transfusion survival rate after surgery. As a result, the deformability-based cell sorter was optimized for efficient margination of mice blood. The channel length, channel aspect ratio, and outlet bifurcation of the deformability-based cell sorter were varied as well as the flow rate to achieve satisfactory stiff cell removal. By optimizing our technology and building an in-vivo model to elucidate the clinical benefit of removing the less deformable RBC subpopulation, we believe we can extend blood's shelf life and minimize transfusion-related risks associated with blood storage lesions.

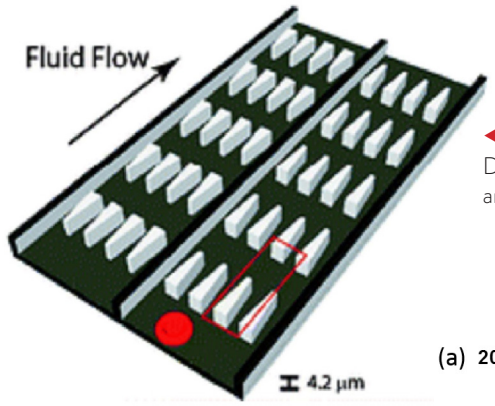

◀ Figure 1: Schematic of the deformability cytometer. Driven by hydraulic pressure, RBCs undergo repeated and extensive deformation in the channel.

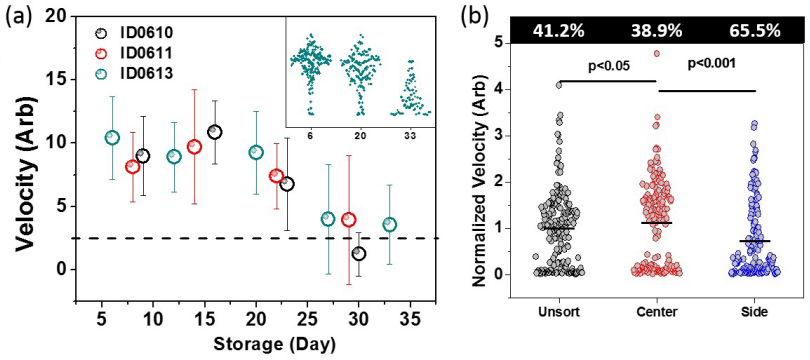

▶ Figure 2: (a) Changes in RBC over prolonged storage time. (b) RBC deformability after margination device sorting.

FURTHER READING

- S. Huang, H. W. Hou, T. Kanias, J. T. Sertorio, H. Chen, D. Sinchar, M. Gladwin, and J. Han, "Towards microfluidic-based depletion of stiff and fragile human red cells that accumulate during blood storage," *Lab on a Chip*, vol. 15, no. 2, pp. 448-58, 2015.
- S. Huang, H. W. Hou, T. Kanias, J. T. Sertorio, H. Chen, M. Gladwin, and J. Han, ""Microfluidic Blood Sorting for Improved Blood Quality over Prolonged Storage," presented at Biomedical Engineering Society Annual Meeting, San Antonio, TX, 2014.
- S. Huang, "Microfluidic Deformability Cytometer for Red Blood Cells," Doctoral thesis, Massachusetts Institute of Technology, Cambridge, 2014.

Single-Cell Study on the Role of ADAM17 in Cancer Drug Resistance

L. Wu, A. M. Claas, D. A. Lauffenburger, J. Han
Sponsorship: Biosystems & Micromechanics IRG, Singapore-MIT Alliance for Research and Technology

Pericellular protease activity, a key component of autocrine signaling, is known to impact the microenvironment of individual cells. Mounting evidence exists for the significant implications of ADAMs, a typical kind of pericelluar protease, in various pathologic settings. However, resulting from the broad substrate specificity of ADAMs, there is a debate over the role of ADAMs in the development of cancer drug resistance. On one hand, the elevated protease-mediated shedding of growth factor ligands have been observed in some resistant cancer cells and shown to be responsible for their resistance by activating an alternative pathway to bypass the specific blockage of the original drug. On the other hand, ADAM proteases shed receptor tyrosine kinases (RTKs) from cell surfaces in addition to growth factor ligands. In cancer cells treated with kinase inhibitors, the activity levels of ADAMs are low, and thus the subsequent RTK shedding is also reduced, leading to RTK accumulation on cell surface. The accumulated RTKs have been shown to enhance the downstream activation of compensatory kinase signaling and confer resistance against specific kinase inhibition. Therefore, it is likely that the variability in ADAM activity of individual cells might have an impact on whether and through which mechanisms each cancer cell can develop resistance to certain drugs. Single-cell measurement of ADAM protease activity is essential to verify this hypothesis.

We have recently developed a microfluidic platform for single-cell measurement of pericellular protease activity. As Figure 1 shows, the designed platform consists of two pieces: a microwell-patterned piece for cell culture (bottom piece) and a 2-layer piece (top piece) acting as an actuatable lid. During each measurement, assay buffer containing FRET-based protease substrate would be introduced into the flow chamber formed between these two pieces. The control channel would then be pressurized to confine substrate and cells within individual microwells. Time-lapse fluorescence imaging would monitor the fluorescence generated by protease-mediated substrate cleavage in real time. Besides, our approach of protease measurement does not require lysis of target cells, which allows us to interrogate the same alive target cell repeatedly to study its temporal behavior upon drug challenge and correlate its protease response with other drug-induced cellular phenotypes, such as morphology, migration, and survival. In the current on-going study, we are utilizing this microfluidic platform to measure the single-cell protease activity distribution of a cancer cell population at different time points across the resistance development process. The evolution profile of single-cell protease activity would offer prospect for studying the role of pericelluar protease in cancer drug resistance.

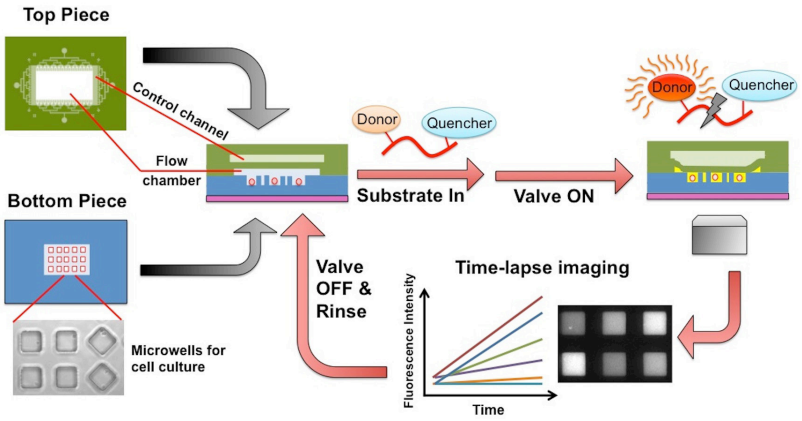

◀ Figure 1: Schematic of single-cell protease assay platform and assay procedure. Upon assembly of top and bottom pieces, assay buffer containing FRET-based substrate is introduced to each microwell via flow chamber, followed by pressurizing control channel to isolate microwells into discrete compartments. Time-lapse fluorescence imaging provides measurement of protease-mediated substrate cleavage. At end of assay, cell-loaded microwell array could be rinsed with fresh assay buffer for subsequent repeated measurements.

FURTHER READING

- B.-B. S. Zhou, M. Peyton, B. He, C. Liu, L. Girard, E. Caudler, Y. Lo, F. Baribaud, I. Mikami, N. Reguart, G. Yang, Y. Li, W. Yao, K. Vaddi, A. F. Gazdar, S. M. Friedman, D. M. Jablons, R. C. Newton, J. S. Fridman, J. D. Minna, and P. A. Scherle, "Targeting ADAM-mediated ligand cleavage to inhibit HER3 and EGFR pathways in non-small cell lung cancer," *Cancer Cell*, vol. 10, no. 1, pp. 39–50, July 2006.
- M. A. Miller, A. S. Meyer, M. T. Beste, Z. Lasisi, S. Reddy, K. W. Jeng, C.-H. Chen, J. Han, K. Isaacson, L. G. Griffith, and D. A. Lauffenburger, "ADAM-10 and -17 regulate endometriotic cell migration via concerted ligand and receptor shedding feedback on kinase signaling," in *Proc. National Academy of Sciences of the United States of America*, 2013, vol. 110, no. 22, pp. E2074–E2083.
- L. Wu, A. M. Claas, A. Sarkar, D. A. Lauffeburger, and J. Han, "High-throughput protease activity cytometry reveals dose-dependent heterogeneity in PMA-mediated ADAM17 activation," *Integrative Biology*, 2015, vol. 7, no. 5, pp. 513-524.

A Nanofluidic Device for Size-Based Protein Concentration and Separation

S. H. Ko, J. Han
Sponsorship: DARPA

Size-based separation of proteins (e.g. sodium dodecyl sulfate polyacrylamide gel electrophoresis (SDS-PAGE) (is widely used to check the purity of protein drugs in the pharmaceutical industry and to ensure the lack of toxic impurities (e.g., protein aggregates). Liquid gel electrophoresis has been automated in a microfluidic platform but still requires polymeric sieving matrices that can increase technical complexity, preventing implementation of truly portable, on-site drug purity and efficacy tests. We have designed a single-step, one-inlet-one-outlet protein analysis device to both concentrate and separate proteins based on size. This system is simple and straightforward to operate; it enhances the detection sensitivity, matching or exceeding that of the standard technique.

Our design relies on angled nanofilters and enables both protein concentration and separation with a simple one-step introduction of analytes. Each molecule with a certain size has its own distinct trajectory determined by a configurational entropic barrier. Proteins are first manipulated to form a narrow, concentrated band, followed by size-based separation for analysis (Figure 1). The key innovation here is the integrated concentration region, which not only defines the "launching band" for protein separation but also carries out significant concentration to improve the overall detection sensitivity, even in a thin nanofluidic channel (~100 nm). To check the enhancement of detection sensitivity, we measured the limit of detection (LOD) and concentration factor with different concentrations of a protein (BSA). Figure 2 shows that LOD (80ng/mL) and concentration factor (~100 fold) were achieved. This is a higher detection sensitivity than the silver staining method (1~10ng of protein required per ~10μL loading volume).

We have designed and implemented a new nanofilter system, which would allow simultaneous continuous-flow preconcentration and separation. The efficiency and purpose of the device are determined by only geometry design, such as nanochannel depth, angle, nanofilter period, and inlet width. In addition, unlike previously developed nanofluidic sieving devices, this device enables effective separation and detection for low concentration biomolecules, opening the possibility for its use as a substitute for SDS-PAGE. We believe the device demonstrated here can be used as a point-of-care drug (biologics) efficacy monitoring system, due to its operational simplicity, robustness (no chemical degradation of gels), and minimal sample use (~1 nL of sample volume). The high detection sensitivity of the system could enable detection of low-level impurities in biological drugs that can lead to significant toxicity in patients. In addition, similar systems can be used to measure activity (binding affinity) of the biological drugs as well.

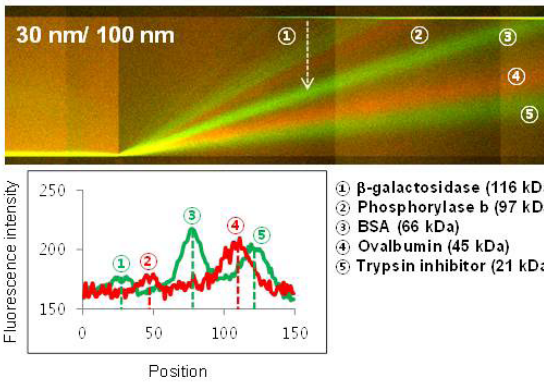

▲ Figure 1: Demonstration of five proteins separation (each protein concentration: 66 μg/mL. SDS-denatured proteins). Fluorescence profiles are measured along white dotted line.

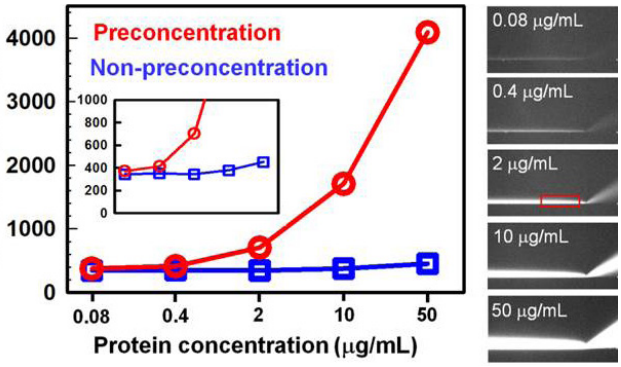

▲ Figure 2: Quantification of LOD and preconcentration factor with different concentration proteins (0.08 μg/mL ~ 50μg/mL).

FURTHER READING

- S. H. Ko and J. Han, "One-Step Protein Analysis Using Slanted Nanofilter Array," in *Proc. 18th International Conference on Miniaturized Systems for Chemistry and Life Sciences*, 2014, pp. 2417-2419.
- M. Yamada, P. Mao, J. Fu, and J. Han, "Rapid Quantification of Disease-Marker Proteins Using Continuous-Flow Immunoseparation in a Nanosieve Fluidic Device," *Analytical Chemistry*, vol. 81, pp. 7067-7074, 2009.

Continuous Biomolecule Preconcentration Using Ion Concentration Polarization

T. Kwon, S. H. Ko, J. Han
Sponsorship: DARPA, Samsung Scholarship

A number of research groups have developed polydimethylsiloxane (PDMS) microfluidic biosensor chips in the past decade. The main advantages of these microfluidic chips include disposability, relatively low cost, and low sample volumes. Preconcentration of target samples can enable faster reaction between target and sensing molecules and improve detection sensitivity of biosensor devices.

In this context, our group demonstrated an enzymatic assay with faster reaction rate and high detection sensitivity in a plug-type concentrator using ion concentration polarization (ICP). When potential difference is applied across an ion-selective membrane, ions are enriched in cathodic side while they are depleted in anodic side. Then, as described in Figure 1, charged molecules cannot pass through this depletion region (charge barrier), and we can concentrate charged molecules by applying pressure-driven and/or electroosmotic flows. However, in the plug-type concentrator, downstream processing of concentrated samples is limited, and selective concentration of either target or sensing molecules to study reaction kinetics was impossible. Kwak et al. demonstrated a continuous-flow preconcentrator based on ICP. In the future, by utilizing the concept of the continuous preconcentrator, we plan to develop a novel enzyme assay chip capable of continuous preconcentration of target samples.

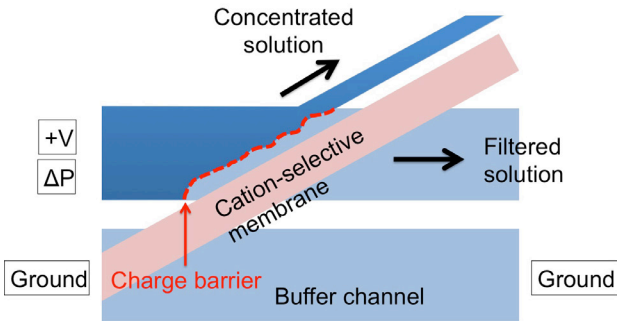

◀ Figure 1: Continuous preconcentration of charged molecules in the microfluidic channel. The charge barrier is formed near cation-selective membrane with voltage difference applied. The concentrated solution is diverted to the upper narrow channel..

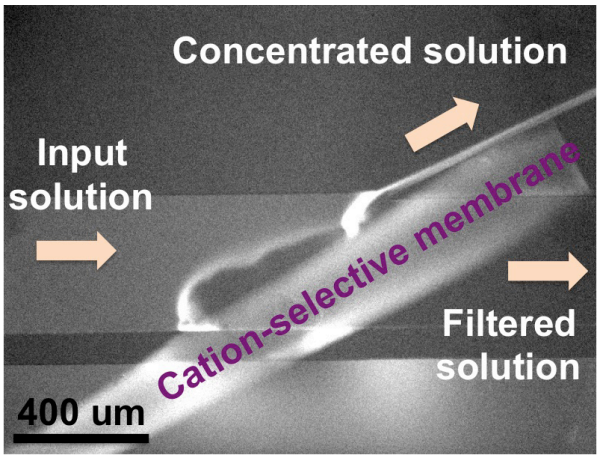

▶ Figure 2: The example of continuous preconcentration of charged molecules. Negatively charged fluorescein isothiocyanate (10 ug/mL) was continuously preconcentrated in the microfluidic channel.

FURTHER READING

- S. J. Kim, Y.-A. Song, and J. Han, "Nanofluidic concentration devices for biomolecules utilizing ion concentration polarization: theory, fabrication, and applications," *Chemical Society Reviews*, vol. 39, pp. 912-922, Mar., 2010.
- J. H. Lee, Y.-A. Song, S. R. Tannenbaum, and J. Han, "Increase of reaction rate and sensitivity of low-abundance enzyme assay using micro/nanofluidic preconcentration chip," *Analytical Chemistry*, vol. 80, pp. 3198-3204, May., 2008.
- R. Kwak, S. J. Kim, and J. Han, "Continuous-Flow Biomolecule and Cell Concentrator by Ion Concentration Polarization," A*nalytical Chemistry*, vol. 83, pp. 7348-7355, Oct., 2011.

Microfluidic Cell Pairing for Studying Immunity

B. Dura, J. Voldman
Sponsorship: Frank Quick Faculty Research Innovation Fellowship

The immune system is tasked with mounting and maintaining protective responses against a wide range of threatening conditions. An effective response requires direct cell-cell interactions, where the ligation of immunoreceptors together with co-stimulatory and co-inhibitory molecules initiates a signaling cascade that promotes immune cell activation and governs a diverse set of developmental (selection, proliferation, differentiation, etc.) and functional immune responses (cytolysis, cytokine secretion, antibody production, etc.). Methods to study these immune cell interactions, however, suffer from limited throughput and a lack of control over cell pairing. Moreover, conventional assays generally depend on bulk co-cultures where the ambiguous nature of cell-cell interactions (number of interacting partners, duration and timing of contacts, etc.) obscures the interpretation of results.

To address these shortcomings, we developed a microfluidic cell-pairing platform that captures and pairs hundreds of lymphocytes using a deterministic back-and-forth cell-loading procedure (Figure 1a-d). This technique creates homogeneously defined one-to-one interactions with enduring contacts, simultaneous timings, and identical contact durations, thereby preventing any variation that would have been otherwise introduced into responses due to the differences in interaction parameters, as would occur in bulk co-cultures. Controlled initiation of interactions further enable examination of the immune cell interaction dynamics from the very onset. The soluble environment around the cell pairs can be controlled by media exchange without disturbing cellular interactions, which enables sequential probing of cell pairs through on-chip stimulation, staining, and fixation protocols. Using these features, we demonstrated, for the first time, dynamic pairwise-correlated measurements over hundreds of cell pairs at the single-cell level in a single experiment (Figure 1e). We further used our devices to monitor early activation dynamics and molecular events during lymphocyte activation, to track cellular response histories upon sequential stimulation, and to characterize the relationship between lymphocyte receptor affinities and early activation dynamics in two lines of melanoma antigen TRP1-specific transnuclear mouse models. Together, our data establish the microfluidic cell pairing platform as a valuable tool for investigation of cell–cell interactions in immunology.

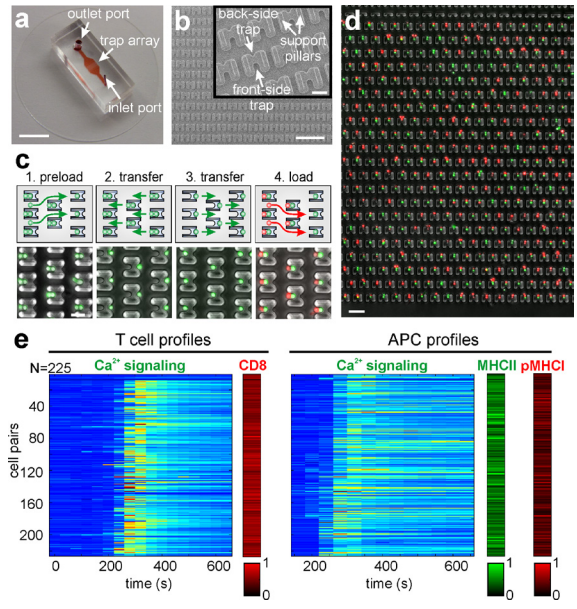

◀Figure 1: Microfluidic device for immune cell pairing. (a) Image of microfluidic cell-pairing device. Channels and trap array are red. (b) SEM image of cell trap array. (c) Four-step cell loading and pairing protocol. (d) Overlaid phase contrast and fluorescence images show primary mouse lymphocytes stained with DiI (red) and DiO (green) membrane dyes paired in traps. (e) Interaction profiles of OT-I CD8 T cell–APCs compiled over 225 pairs showing raw data set including calcium mobilization and expression of CD8 (T cell), MHCII (APC), and pMHCI (APC) surface molecules. Cell pair responses were arranged based on T-cell calcium responses, i.e., non-responders vs. responders. Response profiles corresponding to non-responder T cells are separated from responders using black line. Range for calcium heat maps: 0 (low)—2.5 (high) where blue indicates low calcium, red indicates high. Scale bars: (a) 5 mm, (b) 100 μm, 20 μm (inset), (d) 50 μm.

FURTHER READING

- B. Dura, S. K. Dougan, M. Barisa, M. M. Hoehl, C. T. Lo, H. L. Ploeghand, and J. Voldman, "Profiling lymphocyte interactions at the single-cell level by microfluidic cell pairing," *Nature Communications* vol. 6, 2015. doi:10.1038/ncomms6940.

Iso-Dielectric Separation of Cells and Particles

H. W. Su, L. Liu, J. Voldman
Sponsorship: DARPA

The development of new techniques to separate and characterize cells with high throughput has been essential to many of the advances in biology and biotechnology over the past few decades. We are developing a novel method for the simultaneous separation and characterization of cells based upon their electrical properties. This method, iso-dielectric separation (IDS), uses dielectrophoresis (DEP, the force on a polarizable object) and a medium with spatially varying conductivity to sort electrically distinct cells while measuring their effective conductivity (Figure 1). It is similar to iso-electric focusing, except that it uses DEP instead of electrophoresis to concentrate cells and particles to the region in a conductivity gradient where their polarization charge vanishes. Recently, we have applied IDS to characterize electrical profile of leukocytes for monitor sepsis. One challenge in characterizing blood cells is that the cells change their state very quickly. Delay between blood draw and analysis could introduce inaccuracy. To address this problem, we have started building a portable IDS system for real-time monitoring of cells (Figure 2a). We have designed a circuit board to generate electrical signal with sufficient voltage and current output to drive IDS system (Figures 2b & 2c). A microcontroller such as Arduino or Raspberry Pi will communicate with the DDS and the gain amplifier, allowing control of the voltage and frequency of the signal.

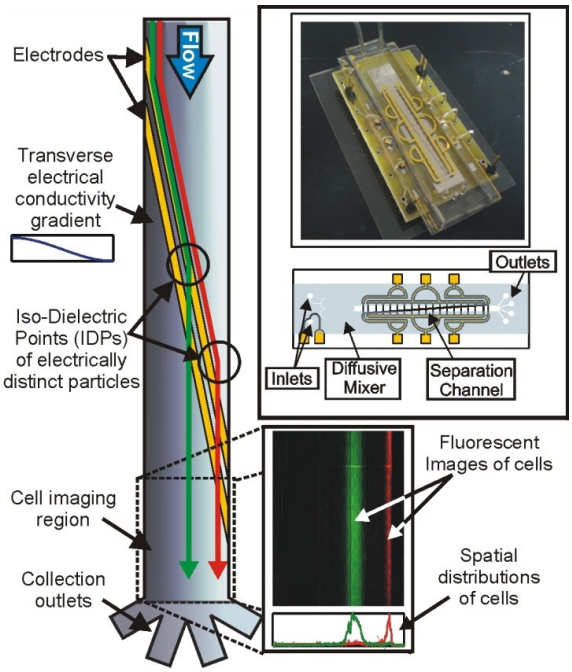

▲ Figure 1: IDS microfluidic device used to measure electrical properties of the cells. The spatial conductivity gradient makes cells with different electrical properties pass through the electrodes at different positions (isodielectric point - IDP).

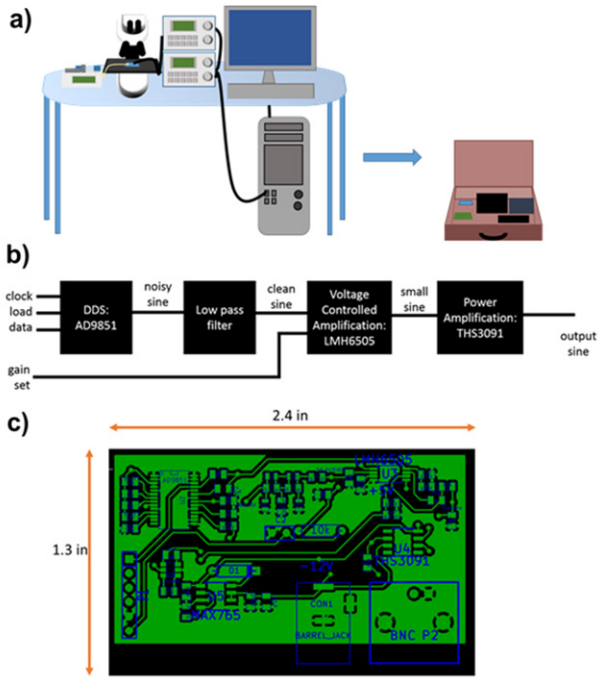

▲ Figure 2: Development of portable IDS system. (a) The goal is to replicate the components of the IDS system and fit into a suitcase. (b) Block diagram of signal generator for the electrical system of the portable IDS. (c) PCB layout of the electrical system.

FURTHER READING

- H. A. Pohl and J. S. Crane, "Dielectrophoresis of cells," *Biophysical Journal*, vol. 11, no. 9, pp. 711-727, Sept. 1971.
- M. D. Vahey and J. Voldman, "An Equilibrium Method for Continuous-Flow Cell Sorting Using Dielectrophoresis," *Analytical Chemistry*, vol. 80, no. 9, pp. 3135-3143, Mar. 2008.
- H. W. Su, J. L. Prieto, L. Wu , H. W. Hou, M. P. Vera, D. Amador-Munoz, J. L. Englert, B. D. Levy, R. M. Baron, J. Han, and J. Voldman, "Monitoring Sepsis Using Electrical Cell Profiling in a Mouse Model," presented at 18th International Conference on Miniaturized Systems for Chemistry and Life Sciences, San Antonio, Texas, 2014.

Cell-Based Sensors for Measuring Impact of Microsystems on Cell Physiology

S. Varma, J. Voldman
Sponsorship: National Institutes of Health

The use of microsystems to study and manipulate cells has grown significantly over the past years. With this increase in usage, however, there is also a growing concern regarding the impact of microsystems on cell physiology. Specific molecular biology assays used to examine this concern are typically challenging to implement in microsystem environments. This difficulty limits device users to phase microscopy-based assessments which although convenient, can only convey gross-level physiology, and are non-specific to cell stresses. To this end, we have developed cell-based sensors that emit fluorescence when specific cell stress pathways are activated in microenvironments. This approach does not require large cell numbers, additional reagents, or sophisticated measurement equipment. Additionally, this live-cell assay now allows for quantifiable monitoring of specific cell stress pathway activations through the convenience of fluorescence microscopy (Figure 1A).

Using an easy-to-culture and commonly used NIH3T3 cell line, we developed three types of cell-sensors. Specifically, we created a sensor to assess DNA damage in microsystems, which fluoresces in red (RFP) when the relevant p53-p21 DNA damage pathway is activated. To assess cell stress due to electro-thermal effects, we re-engineered our existing heat shock pathway sensor to express RFP as the activation color. Similarly, we have created a novel fluid shear stress (FSS) cell-sensor for quantifying physiological stresses due to ubiquitously found fluid flows in microsystems. In this case RFP turns on when FSS initiates transcription of a mechanosensitive protein: Early Growth Factor-1 (EGR-1). We verified the functionality of all sensors by chemical induction of their respective pathway and noted RFP induction through microscopy (Figure 1B). We further validated sensor response to its relevant physical stressors: DNA damage sensor to UV (Figure 2A) and EGR-1 sensor to FSS (Figure 2B). We successfully measured the mean fold induction of RFP fluorescence (MFIR) through flow cytometry, verifying sensor utility. With these sensors, the microsystems community can now easily measure stress activation within their device environments and design systems best suited for cell health.

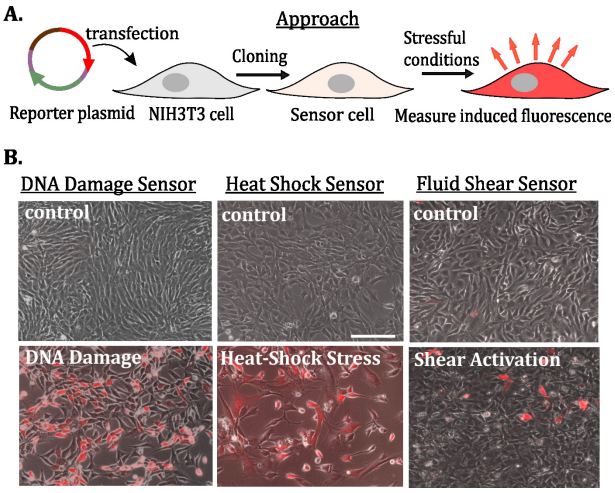

▲Figure 1: A. Approach to creating and using cell sensors. B. Chemical stressors cause respective sensors to fluoresce (lower panels): DNA damage caused by 4 h treatment of methyl methanesulfonate, heat shock caused by 30 min of arsenite treatment, and FSS pathway activation by 24 h of phorbol 12-myristate 13-acetate treatment. Scale: 100 μm.

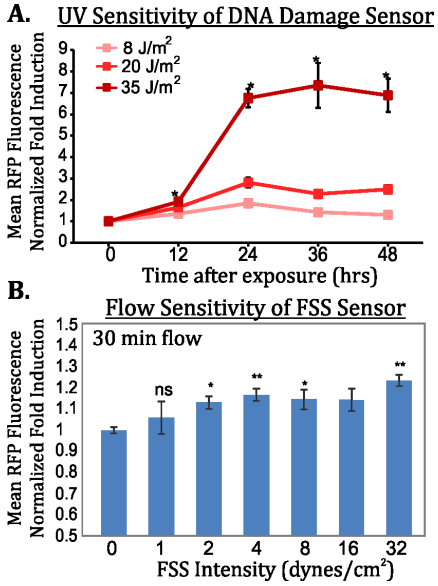

▲Figure 2: Sensor activations through physical stressor exposures. A. UV exposures increase MFIR dynamics for DNA damage sensor. B. Relevant fluid shear stress exposures induce dose- dependent MFIR of FSS sensor.

FURTHER READING

- S. P. Desai and J. Voldman, "Cell-based sensors for quantifying the physiological impact of microsystems." *Integrative Biology*, vol. 3, pp. 48-56, Jan. 2011.
- A. Fendyur, S. Varma, C. T. Lo, and J. Voldman, "Cell-based biosensor to report DNA damage in micro- and nanosystems." *Analytical Chemistry*, vol. 86, no. 15, pp. 7598–7605, July 2014.
- S. Varma and J. Voldman, "A cell-based sensor of fluid shear stress for microfluidics." *Lab on a Chip*, vol. 15, no. 6, pp. 1563-73, March 2015.

Microfluidic Electronic Detection of Protein Biomarkers

D. Wu, J. Voldman
Sponsorship: Maxim Integrated

Immunoassays use antibodies to detect protein biomarkers; these assays have a substantial market and significant clinical importance. However, traditional immunoassays are performed in centralized laboratories using optical methods, which mean results take days and assays cannot be highly multiplexed, in turn increasing patient visits and healthcare costs while decreasing healthcare outcomes. We are developing an all-electronic immunoassay with which we can 1) achieve high-throughput, potentially measuring all protein biomarkers in blood samples; 2) reduce cost by taking advantage of the decreasing cost of silicon electronics; and 3) deliver results to patients before they meet with their physicians.

The biosensor is illustrated in Figure 1: samples are loaded into the microfluidic channel, then antigens specifically bind to antibodies on intergidital electrodes, and finally the presence of antigens is captured by capacitance change due to the binding. To immobilize antibodies, the elctrode was modified using self-assembled monolayers and specific binding between biotin and streptavidin. In our last report, we showed that capacitance measurement can indicate specific binding of protein; but instead of their behavior in a standard buffer, the antigens in practice are in serum or blood whose pH and ionic strength varies from person to person. Therefore we studied the influence of pH and ionic strength. The result (Figure 2) shows capacitance change caused by either pH change or ionic strength variation, as specific protein-binding did; the reasons may be that ionic strength variation altered the double layer capacitance, while the pH change altered the charges on proteins. However, different from capacitance change by protein binding, the change by ionic and pH variation is reversible, which means if we bring them to the original value, the capacitance also recovers. This result suggests that as long as we measure the capacitance before and after protein binding in the same buffer, the capacitance change indictes protein binding, but not ionic and pH variation.

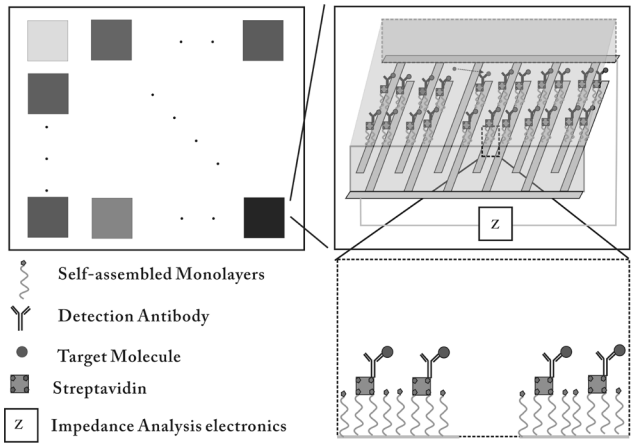

▲ Figure 1: (a) The illustration of multiplexed all-electronic biosensors. (b) The illustration of one pixel of the sensor. (c) The cross section of one pixel.

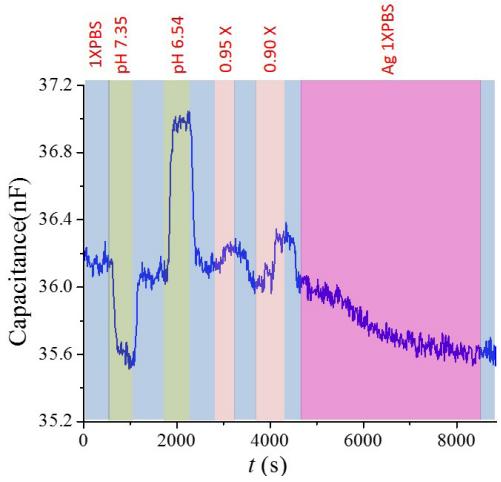

▲ Figure 2: Influence of pH and ionic strength on the sensor signal. The pH of 1X PBS was measured to be 7.04.

Ultrasound-based Cytometry: Absolute Concentration Measurement of Microparticles in Fluid

J. H. Lee, B. W. Anthony, D. S. Boning

The ability to measure the concentration of small particles in a medium has a wide range of applications: laboratory instruments that measure cell concentrations in samples, medical tests that measure red blood cell concentration in blood (hematocrit) or white blood cell concentration in body fluids, and even food industry applications such as measuring yeast concentration in beer and wine. The noninvasiveness of ultrasound makes it especially attractive for medical application. When ultrasound frequency is sufficiently high that the wavelength is similar to the size of the scatterer and the sample is dilute, individual scatterers can be distinguished in the image. While the number of scatterers can be simply counted (Figure 1), quantifying the volume being analyzed by the image is challenging because the exact slice thickness of the image is unknown.

The proposed method estimates the slice thickness of the image by extracting the spread of individual scatters from an ultrasound image generated with a mechanically scanned disk single element transducer. Since a circular transducer has identical azimuthal and elevation beam shape, the resulting slice profile of a linearly scanned transducer is identical to the azimuthal beam shape. The method estimates the beam shape from the spread function of each scatterer, which is a combined result of the transducer point spread function and properties of the scatterer such as size and acoustic impedance. The concentration measurement using the proposed method is compared to the hemocytometer in Figure 2.

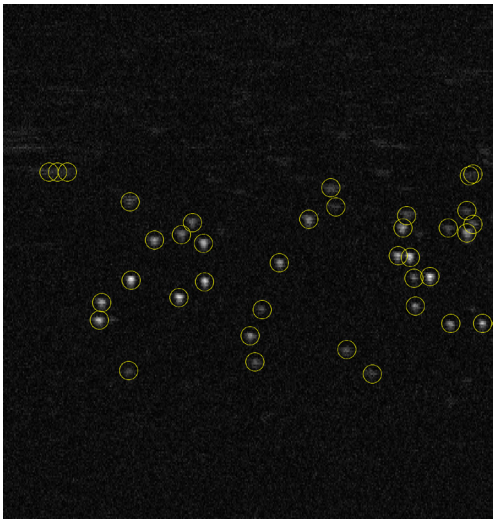

▲ Figure 1: B-mode image of 10-um polystyrene particles suspended in distilled water acquired with a linearly scanned 75-MHz spherically focused transducer.

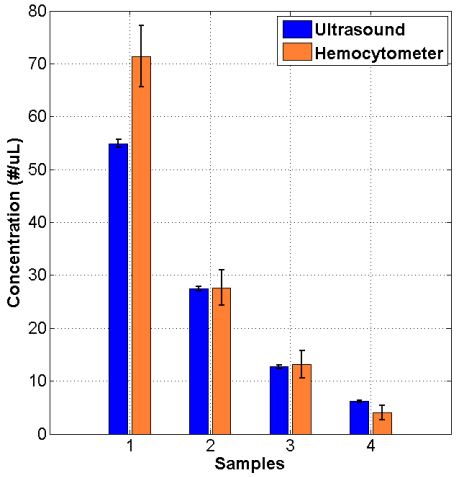

▲ Figure 2: Concentration measurement result comparison between the ultrasound-based method and the hemocytometer. Our proposed method shows good agreement with the existing methods.

FURTHER READING

- A. S. Tunis, R. E. Baddour, G. J. Czarnota, A. Giles, A. E. Worthington, M. D. Sherar, and M. C. Kolios, "Using high frequency ultrasound envelope statistics to determine scatterer number density in dilute cell solutions," in *IEEE Ultrasonics Symposium*, 2005, vol. 2, pp. 878–881.
- K. P. Mercado, M. Helguera, D. C. Hocking, and D. Dalecki, "Estimating Cell Concentration in Three-Dimensional Engineered Tissues Using High Frequency Quantitative Ultrasound," *Ann. Biomed. Eng.*, vol. 42, no. 6, pp. 1292–1304, Mar. 2014.

Electrochemical Sensors for Monitoring Secreted Cardiac Markers from a Heart on a Chip

D.-J. Kim, S. R. Shin, Y. S. Zhang, A. Silvestri, T. Kilic, J. Aleman, H. Alhadrami, R. Riahi, M. R. Dokmeci, A. Khademhosseini
Sponsorship: Defense Threat Reduction Agency

Microfluidic organs-on-a-chip platforms are finding promising applications both in drug screening studies as well as in fundamental biological investigations. Microscale bioreactors as shown in Figure 1(a) are designed to incorporate organoid constructs for long-term cell culture periods in which the organoids are intended to recapitulate the counterparts in the human body. The microenvironment of the bioreactors needs to be monitored to assess the functionality of the organoids. Since biomarker secretion is correlated with many cell functions or dysfunctions, micro-scale analytical tools enabling real-time monitoring and quantitative detection of proteins in vitro is of great importance. It is believed that microfabrication techniques can be utilized to create these microscale biochemical sensors, which can be connected to the microfluidic bioreactors for sensing in small volumes with high precision. Electrochemical biosensors have numerous attractive features including their miniature size, scalability, ease of use, wide sensitivity range, and outstanding selectivity. Here, an electrochemical sensing module was developed and evaluated for detection of secreted biomarkers from cardiac organoids. Immobilization methods were developed with covalent bonding to create stable immobilization of receptors such as antibodies and aptamers onto the surfaces of electrodes. Furthermore, processes for regenerating the surfaces of electrodes were devised to achieve continual monitoring using these devices.

The microelectrodes were integrated into the microfluidic chips as shown in Figure 1(b). The fabrication of microfluidic chips included a valve layer fabricated from PDMS by replica molding against a SU-8 master, which was bonded to a 40-μm-thick PDMS membrane using air plasma. The fluidic layer was similarly fabricated and bonded with the valve layer, sandwiching the membrane in between. The microelectrode was then bonded with the fluidic layer where the detection area was inside the sensing chamber. A bubble trap was also added to the chip on top of the sensing chamber to capture and remove the bubbles from the system. The working electrode (WE), counter electrode (CE), and reference electrode (RE) were wire-bonded for external connection with a potentiostat. The electrochemical impedance spectroscopy (EIS) was employed as the measurement technique. The surface of the microelectrode was functionalized with aptamers against creatine kinase (CK)-MB prior to detection. The attachment of CK-MB at different concentrations to the microelectrode surface resulted in corresponding charge transfer resistance and showed a linear standard curve from the range of 0.01-100 ng/mL, as shown in Figure 2.

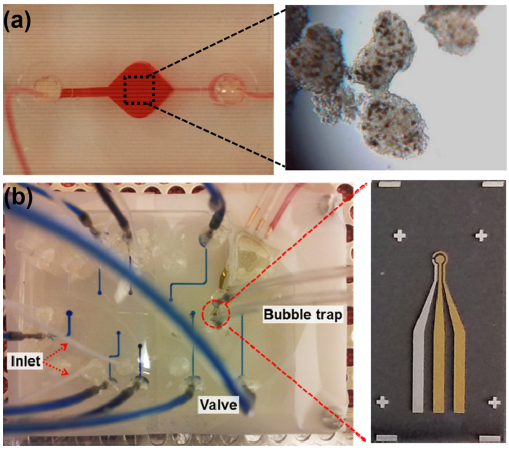

▲ Figure 1: (a) A microscale bioreactor for culturing cardiac organoids. (b) Electrochemical sensors integrated with the microfluidic chip and the photograph of the fabricated microelectrodes.

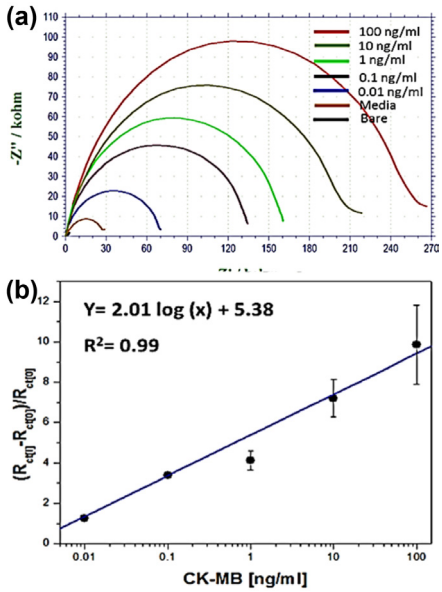

◀ Figure 2: (a) Nyquist plots of impedance spectra and (b) reference curve for CK-MB antigens obtained from ΔRct/Rct(0) measurements captured via electrodes.

FURTHER READING

- S. Selimovic, "Organs-on-a-chip for drug discovery" *Current Opinion in Pharmacology*, vol. 13, pp. 829-833, 2013.
- A. Polini, "Organs-on-a-chip: a new tool for drug discovery," *Expert Opinion on Drug Discovery*, vol. 9, pp. 335-352, 2014.
- Y. S. Zhang, "Seeking the right context for evaluating nanomedicine: from tissue models in petri dishes to microfluidic organs-on-a-chip," *Nanomedicine*, vol. 10, pp. 685-688, 2015.

Graphene Field-Effect Transistor Sensors for Quantitative Real-Time Polymerase Chain Reactions

C. Mackin, M. DeFazio, T. Palacios
Sponsorship: Institute for Soldier Nanotechnologies

Real-time polymerase chain reaction (RTPCR) is a fundamental analytical technique with broad applications in the life sciences (Figure 1). State-of-art RTPCR systems currently rely on fluorescent probes along with bulky and expensive optical systems. Previous works have shown that RTPCR may be accomplished without fluorescent probes and optical detection systems through fine-tuned PCR chemistries and chemical detection using ion-sensitive field-effect transistors (ISFETs). This is accomplished by appropriately reducing the amount of buffer concentration such that proton release during the DNA extension phase is able to modify pH. Because proton release results from nucleotide incorporation during the template DNA extension, pH may be directly related to DNA concentration.

We build on these works by employing graphene field-effect transistor (FET) sensors, which exhibit well-known pH sensitivity. Because graphene FETs consist solely of a graphene channel region contacted by metal leads, this method offers the advantages of a greatly simplified fabrication process and potentially lower cost than its MOSFET-based counterparts. We develop an integrated chip capable of DNA amplification and quantitative real-time DNA detection. The chip contains resistive heating elements, a temperature sensor, and graphene-based FET chemical sensors. Graphene FET sensors quantify DNA concentration via Dirac point shifts induced by proton release during nucleotide incorporation (Figure 2).

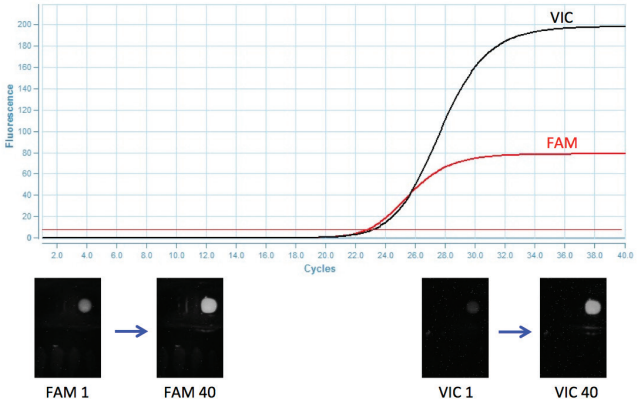

◀ Figure 1: RTPCR experiment using FAM and VIC fluorophores for the detection of a DNA sequence associated with the inability to metabolize clopidogrel, a common antiplatelet medication.

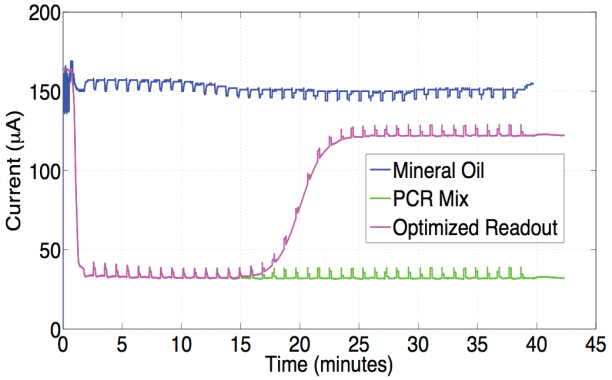

▶ Figure 2: Graphene FET sensor readouts over the course of an RTPCR experiment for mineral oil baseline (blue), PCR mix with excessive buffer concentration (green), and hypothesized readout for optimized buffer concentration (magenta).

FURTHER READING

- C. A. Heid, J. Stevens, K. J. Livak, and P. M. Williams, "Real time quantitative PCR," *Genome Res.*, vol. 6, no. 10, pp. 986–994, Oct. 1996.
- C. Toumazou, L. M. Shepherd, S. C. Reed, G. I. Chen, A. Patel, D. M. Garner, C. A. Wang, C. Ou, K. Amin-desai, P. Athanasiou, H. Bai, I. M. Q. Brizido, B. Caldwell, D. Coomber-Alford, P. Georgiou, K. S. Jordan, J. C. Joyce, M. La Mura, D. Morley, S. Sathyavruthan, S. Temelso, R. E. Thomas, and L. Zhang, "Simultaneous DNA amplification and detection using a pH-sensing semiconductor system," *Nat. Methods*, vol. 10, no. 7, pp. 641–646, 2013.
- B. Mailly-Giacchetti, A. Hsu, H. Wang, V. Vinciguerra, F. Pappalardo, L. Occhipinti, E. Guidetti, S. Coffa, J. Kong, and T. Palacios, "pH Sensing Properties of Graphene Solution-Gated Field-Effect Transistors," *J. Appl. Phys.*, vol. 114, no. 8, p. 084505, 2013.

Chronic, Flexible Electrodes for Interfacing with the Central and Peripheral Nervous System

H. S. Sohal, G. Riggott, E. S. Boyden, R. Desimone
Sponsorship: NIH, McGovern Institute

Micromotion, attributable to the modulus mismatch between the moving brain and electrode materials, is a fundamental phenomenon contributing to generalized electrode failure for chronic brain implants. This failure hampers our ability to dissect neural circuits over chronic experimental paradigms and our ability to produce reliable signals for invasive brain-machine interfaces. We have recently shown that the sinusoidal probe is effective as a chronic implant, providing high-fidelity, stable neural recordings for up to two years with reduced overall gliosis when compared to conventional electrodes (Sohal et al., 2014), perhaps due to its flexibility, and thus intrinsic micromotion-reducing measures. Such measures included a rounded recording tip, a sinusoidal shaft, and a polyimide ball-anchor. The sinusoidal shaft accommodates the brain movement, while the recording sites are anchored in place with the ball anchor. All measures attempt to restrict electrode recording site movement relative to the surrounding brain tissue. The probe is microfabricated out of Parylene-C with WTi recording sites.

The original probe was a proof-of-concept therefore comprised of a limited number of electrode recording sites and restricted to certain lengths. Further, the probes were optimized for chronic recordings in rodents, rather than non-human primates. Now, we have designed and microfabricated the next generation of the sinusoidal probe, substantially increasing the number of recording sites and allowing for multi-depth recording. Lengths of these novel probes, based on the original design, vary from 3-30 mm, allowing for the specific targeting of brain regions in both rodents and non-human primates in highly customizable, 3D arrangements. Further, we have optimized insertion procedures, which may allow for the implantation of more sinusoidal probes using a single carrier, hence minimizing vasculature damage during the insertion process due to repeated brain penetrations. We have also used this process flow to construct differing electrode types for other applications relating to the central and peripheral nervous system in various species.

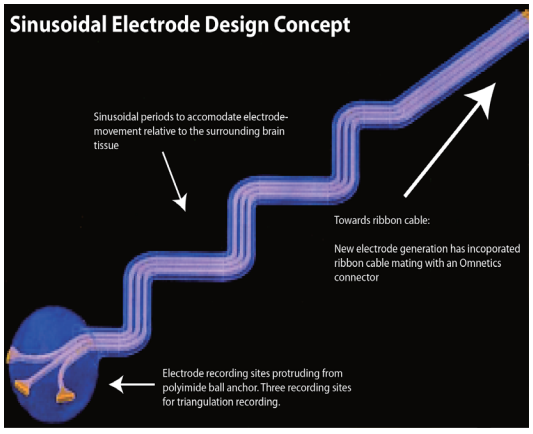

▲ Figure 1: The Flexible Sinusoidal Probe design concept showing the micromotion reducing measures.

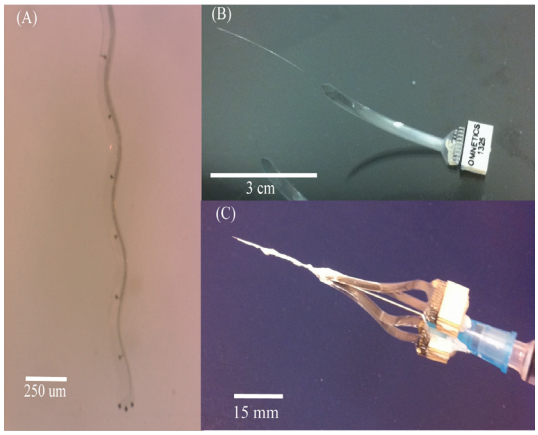

▲ Figure 2: (A) Microfabricated probe, (B) 3-cm-long probe to allow for deep structure targeting, (c) Temporary insertion carrier to allow for the implantation of 4 probes simultaneously with 64 channels of recording

FURTHER READING

- H. S. Sohal, F. Yoshida, K. Payer, G. Riggott, N. Bichot, E. S. Boyden, and R. Desimone, "The sinusoidal probe- towards translation in the non-human primate.," in Proc. 44th Society for Neuroscience Annual Meeting 2014. vol. 659, no. 02, pp. VV22.
- H. S. Sohal, A. Jackson, R. Jackson, K. Vaisilevski, G. J. Clowry, S. N. Baker, and A. O'Neil, "The Sinusoidal Probe: a new approach to improve electrode longevity," *Front. Neuroeng. Special edition*: The chronic challenge - in vivo long-term multisite contact to the central nervous system, 2014.

Reconfigurable Neural Probes for Chronic Electrical Recording

A. Dighe, U. Froriep, M. Sunshine, A. Ievins, P. Anikeeva, C. Moritz, J. Voldman
Sponsorship: National Science Foundation Center for Sensorimotor Neural Engineering

Chronic interfaces with the nervous system are critical for understanding neurobiology as well as for enabling new technologies that could be used in the treatment of various neurological disorders. A major challenge with current brain-computer interfaces is their inability to reliably record single-unit electrical activity over long periods of time (months) due to tissue reaction to foreign objects in the brain. This tissue reaction consists of a sheath of glial cells that encapsulates a neural probe a few weeks after implantation. Here we describe the design of a new neural probe that aims to bypass the body's immune reaction by changing shape once implanted in the brain, thereby providing the ability to chronically monitor neural activity in vivo.

Our reconfigurable electrode consists of a thin polymer probe whose body can be deflected and locked prior to insertion via a dissolvable glue such as polyethylene glycol (PEG), storing mechanical energy in the device legs (Figure 1a). After inserting into the brain and waiting for the initial glial sheath to form (Figure 1b), the device can be triggered by dissolving the glue, causing the recording tip of the device to penetrate into fresh tissue (Figure 1c). Designing the tip dimensions to be small (7-20 μm) should prevent the formation of an additional glial sheath post-triggering. We have demonstrated successful triggering and electrical recordings from this device in an acute setting in the rodent brain (Figure 2). This technology holds promise for creating chronic interfaces for recording stable neural activity.

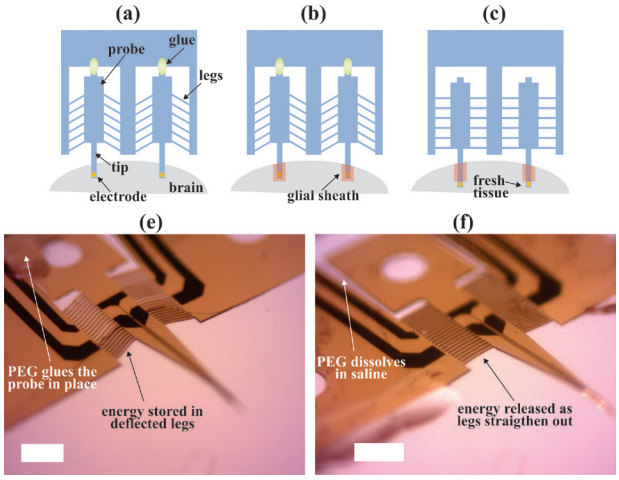

▲ Figure 1: (a) Schematic showing the probe prior to insertion, (b) after glial sheath formation (~weeks), and (c) after dissolving the glue to deploy the probe. (e,f) Photographs of device before and after deployment. Scale bars = 500 μm.

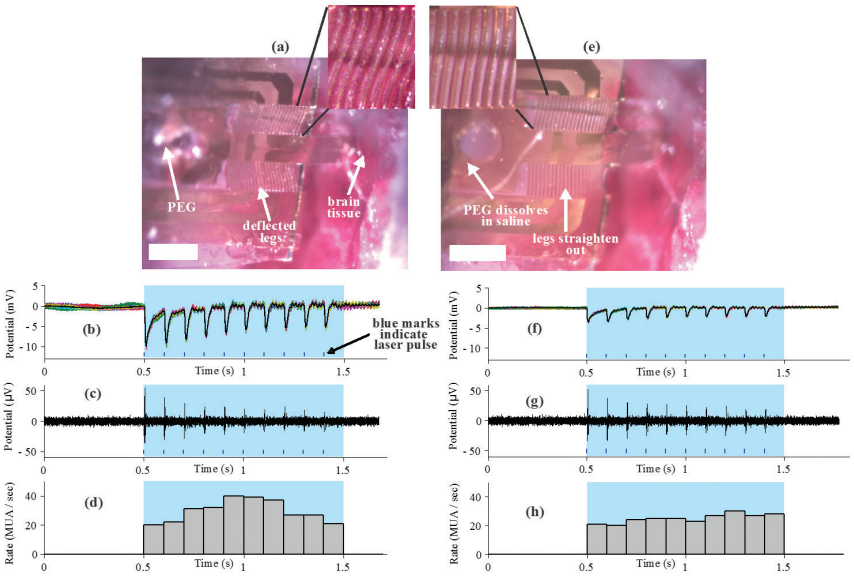

◀ Figure 2: In vivo acute recordings of neural activity in the medial prefrontal cortex of a Thy1-ChR2-YFP optogenetically active mouse. (a) The probe is inserted into the mouse brain (scale bar = 500 μm). (b)-(d) Neural activity is recorded following laser stimulation trains. (e) The probe is deployed. (f)-(h) Neural activity is recorded again in response to the same laser stimulation as in (b)-(d).

FURTHER READING

- A. Dighe, U. Froriep, M. Sunshine, A. Ievins, P. Anikeeva, C. Moritz, J. Voldman, "Development and *in vivo* testing of reconfigurable neural probes for chronic electrical recording," *Proc. Solid-State Sensors, Actuators & Microsystems*, 8-12 June, 2014, Hilton Head, SC, Transducers Research Foundation.
- V. S. Polikov, P. A. Tresco, W. M. Reichert, " Response of brain tissue to chronically implanted neural electrodes," *Journal of Neuroscience Methods*, vol. 184, pp. 1-18, Oct 2005.
- T. D. Y. Kozai, N. B. Langhals, P. R. Patel, X. Deng, H. Zhang, K. L. Smith, J. Lahann, N. A. Kotov, and D. R. Kipke, "Ultrasmall implantable composite microelectrodes with bioactive surfaces for chronic neural interfaces," *Nat Mater*, vol. 11, no. 12, pp. 1065–1073, Dec. 2012.

Probing Neural Circuits with Multifunctional Fiber Probes

A. Canales, X. Jia, C. Lu, U. P. Froriep, R. A. Koppes, C. M. Tringides, J. Selvidge, Y. Fink, P. Anikeeva
Sponsorship: National Science Foundation, McGovern Institute for Brain Research, Draper Laboratory

Our ability to understand and map the temporal dynamics of neural circuits associated with fundamental cognitive processes such as learning or decision-making or to treat the neurological conditions such as major depressive disorder or autism are currently limited by the lack of tools capable of adequately addressing and matching the signaling complexity of the brain. Here we describe an entirely new class of flexible polymer-based multimodal neural communication devices that permit simultaneous *in vivo* optical interrogation, drug delivery and electrophysiological recording at high spatial resolution. For the first time we can employ a combinatorial strategy for chemical and optical communication with neural tissue and obtain a concomitant readout of the neural response in a freely moving mouse via a single flexible optoelectronic fiber probe.

The multimaterial fiber probes are produced in a scalable thermal drawing method that involves the fabrication of a macroscopic model, the preform, which is subsequently heated and stretched into many meters of fiber (Figure 1). The resulting fiber has all of the necessary functions built into it and does not require any post processing. Here we fabricated and evaluated multimaterial fibers based solely on polymers (polycarbonate, PC; conductive polyethylene composite, CPE; and cyclic olefin copolymer, COC) or polymer metal composites. We find that our electrodes possess impedance 0.8-2.5 MΩ, waveguides exhibit losses 0.5-2 dB/cm across the visible spectrum, and micro channels can deliver fluids at rates 1-1000 nl/min. Furthermore, our experiments demonstrate the utility of the fiber probes for neural recording, optogenetic stimulation and infusion of neuromodulatory compounds (such as bicuculline, Figure 2) in transgenic mice expressing channelrhodopsin 2 (ChR2) within the brain and spinal cord. Finally, we show that fiber probes produce minimal foreign body response within the surrounding neural tissue. Our results demonstrate the promise of fiber technology in interfacing with the complexity of the mammalian brain while addressing the tissue compatibility and reliability issues.

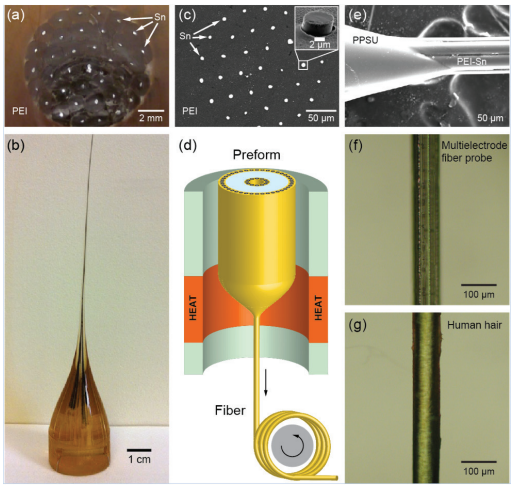

▲Figure 1: (a) Cross section of a multi-electrode preform. (b) Preform drawn into a fiber. (c) Cross sectional SEM image of a fiber probe produced from preform in (a). (d) An illustration of the drawing process. (e) SEM image of a fiber probe exposed from sacrificial cladding. (f), (g) Micrographs of a 7-electrode fiber probe (f) and a human hair (g).

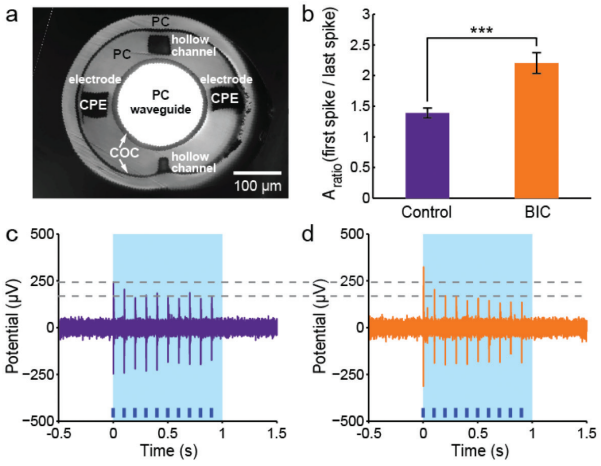

▲Figure 2: Simultaneous recording, optical stimulation, and drug delivery. (a) Cross section of a multimodal fiber probe with CPE electrodes, PC/COC waveguide, and drug delivery channels. (b) Injection of bicuculline changes the amplitude ratio of the optically evoked first and last spikes in the epoch. (c) Pre-bicuculline epoch. (d) Post-bicuculline epoch.

FURTHER READING

- A. Canales, X. Jia, U. P. Froriep, R. A. Koppes, C. M. Tringides, J. Selvidge, C. Lu, C. Hou, L. Wei, Y. Fink, and P. Anikeeva, "Multifunctional Fibers for Simultaneous Optical, Electrical and Chemical Interrogation of Neural Circuits In Vivo," *Nature Biotechnology*, vol. 33, pp. 277-284, 2015.
- C. Lu, U. P. Froriep, A. Canales, R. A. Koppes, V. Caggiano, J. Selvidge, E. Bizzi, and P. Anikeeva, "Polymer Fiber Probes Enable Optical Control of Spinal Cord and Muscle Function In Vivo," *Advanced Functional Materials*, vol. 24, pp. 6594-6600.

Automated Modeling for Large-Scale Arterial Systems

Y.-C. Hsiao, Y. Vassilevski, S. Simakov, L. Daniel
Sponsorship: MIT-Skoltech

Diagnosing medical conditions based on non-invasive (or minimally invasive) measurements requires simultaneous modeling for both (1) local pathological arteries and (2) global arterial networks in order to correlate the available measurements with the actual pathologies. For instance, diagnosing atherosclerosis or an aneurysm requires the detailed understanding of the pressure and flow inside the bifurcation segments. Such information is typically not measurable at pathological sites but may still be attainable if it can be inferred from other measurements. Therefore, it is crucial to develop accurate yet efficient global arterial models such that the correlations between the pathologies and the available measurements can be established. The final diagnosis can be obtained by solving an inverse problem for the pathological parameters, for instance, aneurysm internal diameter, arterial wall thickness, plague stiffness, etc.

For this strategy to be effective, the model for such a large-scale arterial network must be compact, computationally tractable, and field-solver-accurate. We have proposed an innovative technique to automatically generate nonlinear dynamic models using measurement data or simulations results from partial-differential-equation (PDE) solvers, as shown in Figure 1. The generated models are guaranteed numerically stable, both when simulated alone and when interconnected within a network. This stability enables the hierarchical modeling capability, generating models for local sub-networks, such as branches and bifurcations, and interconnecting them to form a global network. An example of such geometry decomposition is demonstrated in Figure 2. This approach allows full exploitation of artery geometries without compromise due to the shape complexity. In addition, because the entire modeling efforts are subdivided into local model generations, the corresponding finite-element problems for generating training data are at a tractable size. Therefore, the fluid dymamics PDEs, such as viscosity and turbulence, can be fully utilized to capture all types of nonlinearities without simplication.

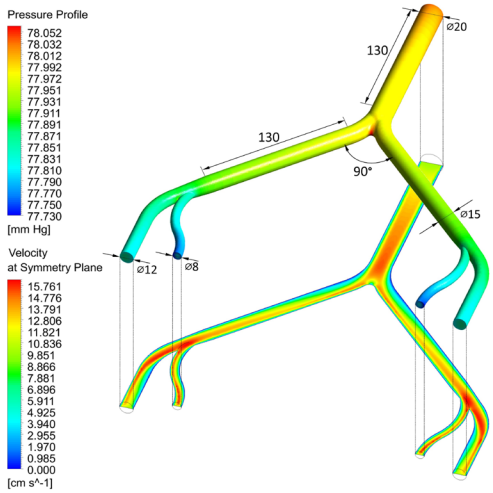

▲Figure 1: Pressure profile (upper) and velocity profile (lower) of the human abdominal aorta and iliac arteries.

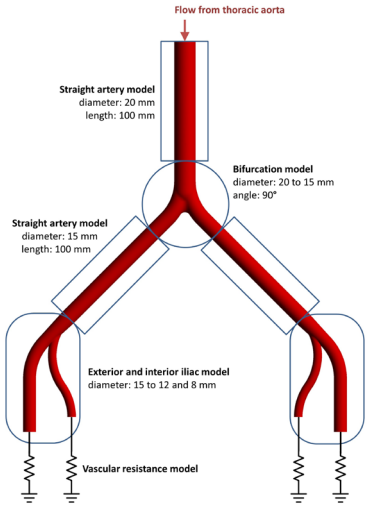

▲Figure 2: Arterial network decomposition into local models. Each model is automatically generated using our proposed algorithm. The simulation of the overall system is accurate, efficient, and guaranteed numerically stable.

FURTHER READING

- B. Bond, T. Moselhy, and L. Daniel, "System identification techniques for modeling of the human arterial system," in Proc. SIAM Conference on the Life Sciences, 2010, pp. 12-15.
- Y.-C. Hsiao and L. Daniel, "Sparse basis pursuit on automatic nonlinear circuit modeling," presented at IEEE International Conference on ASIC (ASICON), Shenzhen, China, Oct., 2013.

MARIE: A MATLAB-Based Open Source MRI Electromagnetic Analysis Software

J. Fernández Villena, A. Polimeridis, J. Cruz Serralles, L. Wald, E. Adalsteinsson, J. White, L. Daniel
Sponsorship: National Institute of Health, Skoltech Initiative on Computational Mathematics

MARIE (MAgnetic Resonance Integral Equation suite) is a numerical software platform for comprehensive frequency-domain fast electromagnetic (EM) analysis of MRI systems. The tool is based on a combination of surface and volume integral equation formulations. It exploits the characteristics of the different parts of an MRI system (coil array, shield and realistic body model), and it applies sophisticated numerical methods to rapidly perform all the required EM simulations to characterize the MRI design. The underlying engine of MARIE is based on integral equation methods applied to the different domains that exist in traditional MRI problems (for example, except in interventional cases, the coil and body occupy separate spaces). The natural domain decomposition of the problem allows us to apply and exploit the best modeling engine to each domain. The inhomogeneous human body model is discretized into voxels and modeled by volume integral equation methods. The homogeneous conductors that form the coil design and shield are tessellated into surface triangles, and modeled by surface integral equation methods. Both models are coupled by applying standard dyadic Green functions. Once the models are generated, fast numerical methods are applied to solve the complete system. A set of nested iterative methods with the appropriate preconditioning is used to solve the effect of each port. Fast Fourier Transform techniques exploit the regularity of the voxelized grid and accelerate the matrix vector products. Depending on the different analysis scenarios, some numerical models or tasks can be pre-computed to accelerate the solution, and many strategies are used to reduce either computational time or memory consumption.

The software runs on MATLAB and is able to solve a complex scattering problem in ~2-3 min. on a standard single GPU-accelerated desktop computer. On the same platform it can perform a frequency sweep of a complex coil in ~3-5 min. per frequency point. Furthermore, it can solve the complete inhomogeneous body and coil system in ~5-10 min. per port, depending on the model resolution and error tolerance required. Intended to be a development platform, it includes a simple and intuitive graphical user interface (see Figure 1 for a snapshot) for standard analysis and a set of well-documented scripts to illustrate how to use the core numerical functions to perform more advanced analyses. The underlying numerical routines can be used to generate standard results, such as the B1+, B1- and E maps presented in Figure 2, or to address other relevant problems, such as the generation of ultimate intrinsic SNR and SAR on realistic body models, fast coil design and optimization, and generation of patient-specific protocols, among others.

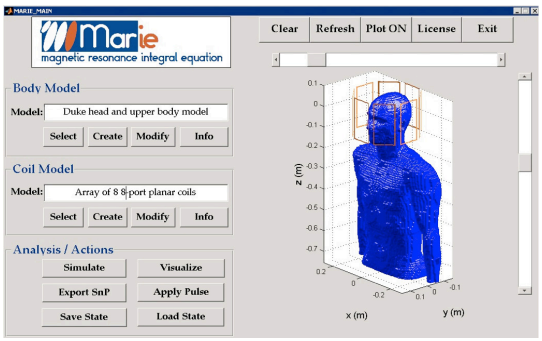

▲ Figure 1: Snapshot of MARIE's graphic user interface with body and coil models loaded, for which the simulation results are shown in Figure 2.

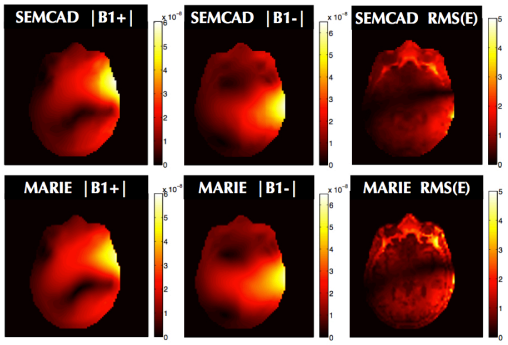

▲ Figure 2: Comparison of the (left) B1+, (center) B1-, and (right) RMS(E) maps for a body model. Top maps are with SEMCAD (SPEAG), bottom with MARIE.

FURTHER READING

- A. G. Polimeridis, J. Fernández Villena, L. Daniel, and J. K. White, "Stable FFT-JVIE solvers for fast analysis of highly inhomogeneous dielectric objects," *Journal of Comp. Physics*, 269:280-296, 2014.
- A. Hochman, J. Fernández Villena, A. G. Polimeridis, L. M. Silveira, J. K. White, and L. Daniel, "Reduced-order models for electromagnetic scattering problems," *IEEE Trans. on Antennas and Propagation*, 62(6):3150-3162, 2014.